VISTA seminar, April, 2022

Nonadiabatic Dynamics, Machine Learning and Time-Resolved Pump-Probe Spectra

Zhenggang Lan

2022.04

South China Normal University

Introduction

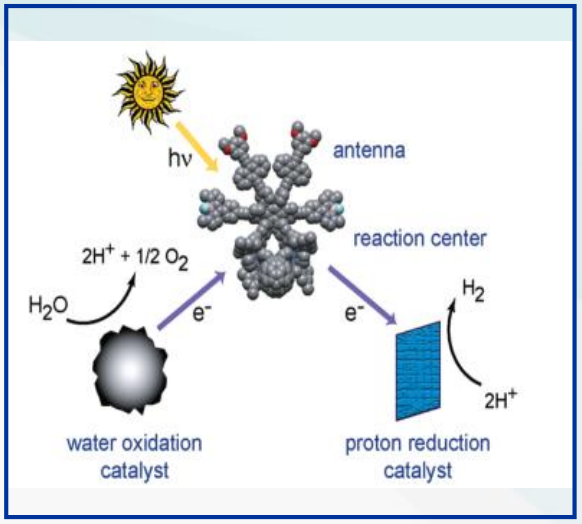

?

$$H\psi = E\psi, \qquad ih\frac{\partial\psi}{\partial t} = H\psi$$

$$\frac{dp_i}{dt} = -\frac{\partial H}{\partial q_i}, \qquad \frac{dq_i}{dt} = +\frac{\partial H}{\partial p_i}$$

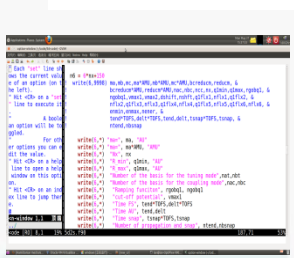

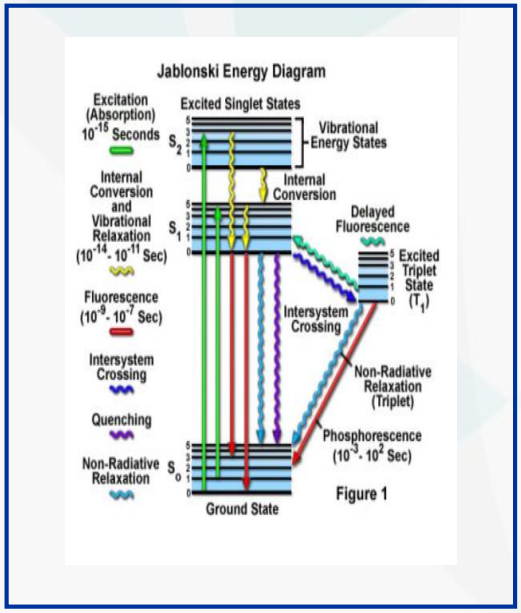

Nonadiabatic dynamics

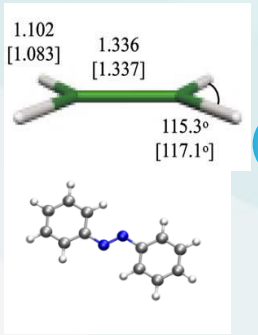

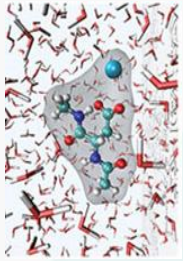

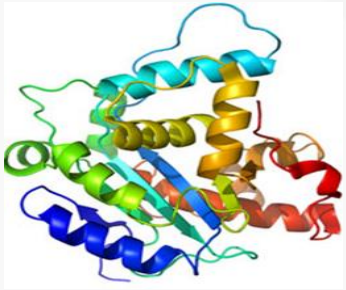

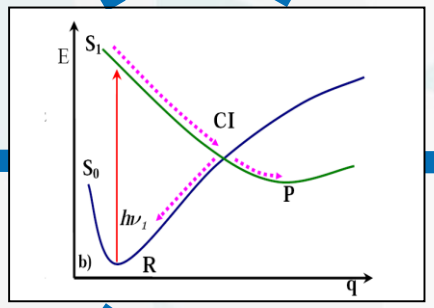

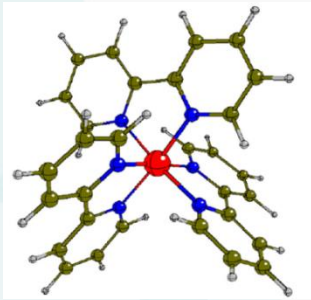

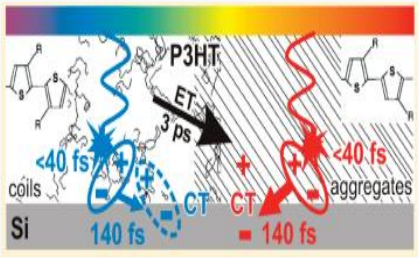

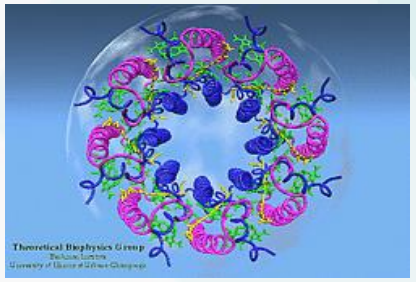

Research highlights

Potential Energy Surfaces

Diabatization

Mixed quantum classical
Quasi-classical
Semiclassical
Dynamics

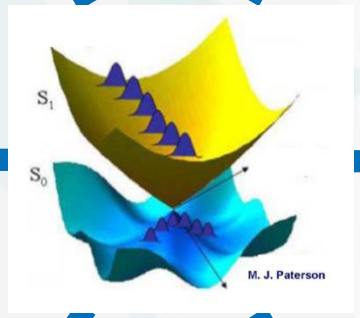

Quantum Wavepacket and Dissipative Dynamics

Machine Learning

Time-resolved spectroscopy

Transient-Absorption Pump-Probe Signals

Pump-probe spectroscopy

Hamiltonian

$$\hat{H}(t) = \hat{H}_M + \hat{H}_F(t)$$

$$\hat{H}_F(t) = -\hat{\boldsymbol{\mu}} \cdot \boldsymbol{E}(t)$$

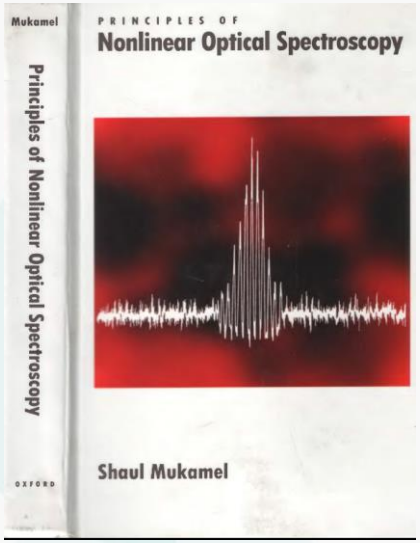

Third-order polarization

$$\boldsymbol{P}^{(3)}(t) = (i)^3 \int_0^\infty dt_3 \int_0^\infty dt_2 \int_0^\infty dt_1 \boldsymbol{E}(t-t_3)\boldsymbol{E}(t-t_3-t_2)\boldsymbol{E}(t-t_3-t_2-t_1)S(t_3,t_2,t_1)$$

$$S(t_3,t_2,t_1) = Tr\{\hat{\boldsymbol{\mu}}^I(t_1+t_2+t_3)[\hat{\boldsymbol{\mu}}^I(t_1+t_2),[\hat{\boldsymbol{\mu}}^I(t_1),[\hat{\boldsymbol{\mu}}^I(0),\hat{\rho}(-\infty)]]]\}$$

$$\hat{\boldsymbol{\mu}}^I(t) = e^{i\hat{H}_M(t-t_0)}\hat{\boldsymbol{\mu}}e^{-i\hat{H}_M(t-t_0)}$$

Pump-probe electronic field

$$\boldsymbol{E}(t) = \boldsymbol{E}_{pu}(t) + \boldsymbol{E}_{pr}(t-\tau)$$

$$\boldsymbol{E}_{pu}(t) = \boldsymbol{\varepsilon}_{pu}E_{pu}(t)e^{i\mathbf{k}_{pu}\mathbf{x}}e^{-i\omega_{pu}t} + \text{c.c.}$$

$$\boldsymbol{E}_{pr}(t-\tau) = \boldsymbol{\varepsilon}_{pr}E_{pr}(t-\tau)e^{i\mathbf{k}_{pr}\mathbf{x}}e^{-i\omega_{pr}t} + \text{c.c.}$$

Pump-probe signal

$$I_{\text{int}}(\tau,\omega_{pr}) = \omega_{pr}\,\text{Im}\left\{\int_{-\infty}^{\infty} dt E_{pr}(t)e^{i\omega_{pr}t}P^{(3)}_{\mathbf{k}_{pr}}(\tau,t)\right\}$$

$$I_{dis}(\tau,\omega) = \omega_{pr}\,\text{Im}\left\{\varepsilon_{pr}(\omega)P^{(3)}_{\mathbf{k}_{pr}}(\tau,\omega)\right\}$$

(1) Gelin, M. F.; Huang, X.; Xie, W.; Chen, L.; Doslic, N. A.; Domcke, W. *J Chem Theory Comput* **2021,** *17*, 2394-2408.

(2) Mukamel, S. Principles of Nonlinear Optical Spectroscopy. **1995**.

GSB, SE and EAS components in TA PP signals

Feynman Diagrams

Ground-State Bleach

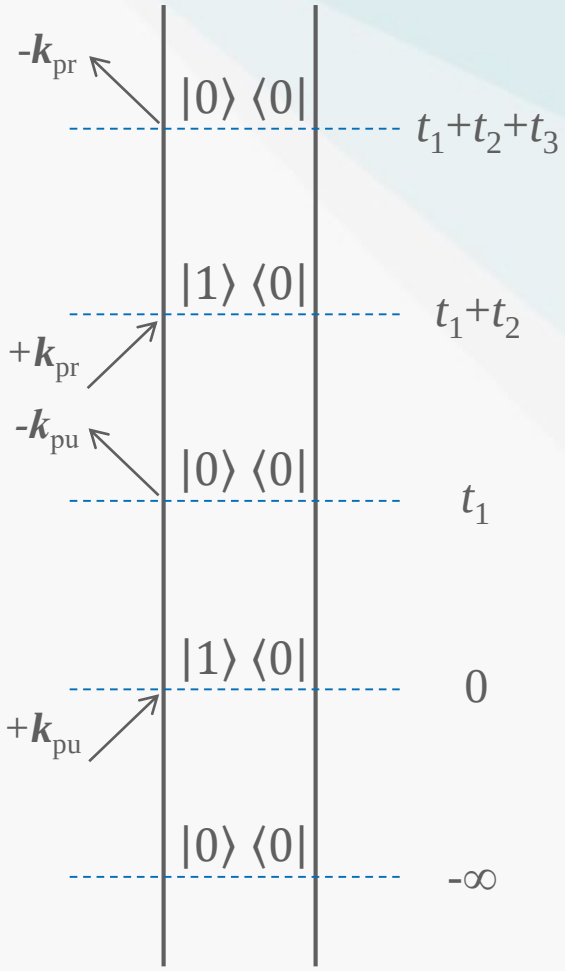

Stimulated Emission

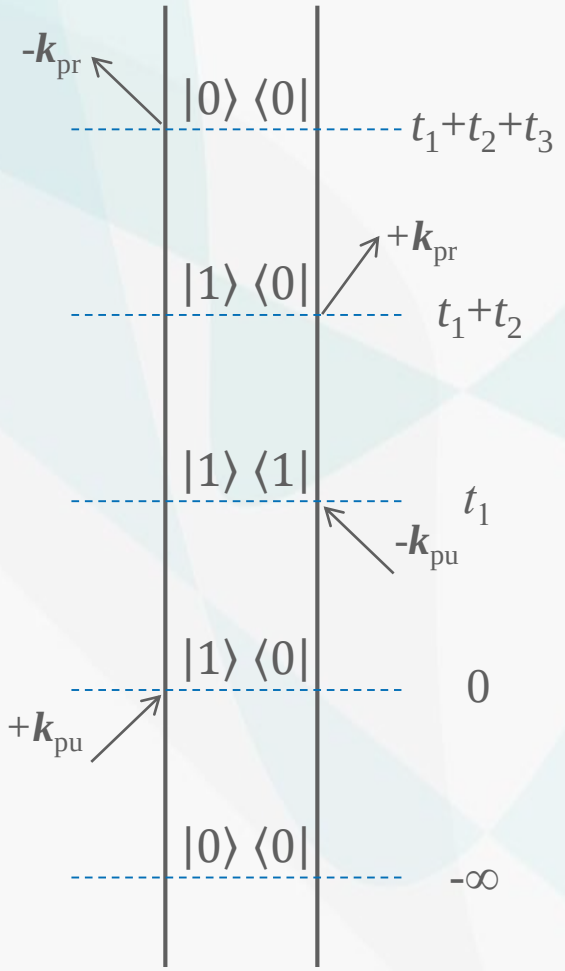

Excited-State Absorption

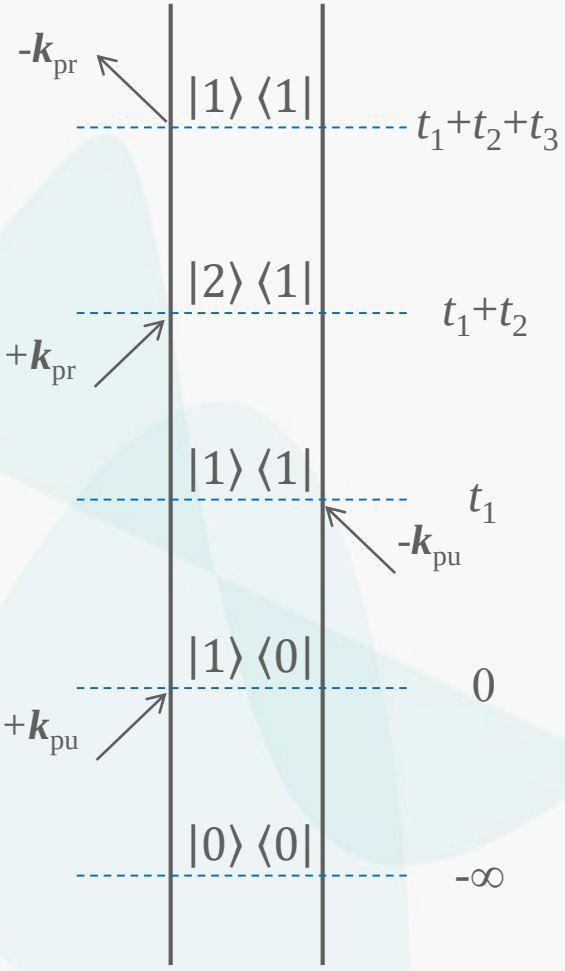

(1) Gelin, M. F.; Huang, X.; Xie, W.; Chen, L.; Doslic, N. A.; Domcke, W. *J Chem Theory Comput* **2021,** *17*, 2394-2408.

(2) Mukamel, S. Principles of Nonlinear Optical Spectroscopy. **1995**.

Doorway-Window Approximations of Signals

Doorway-window approximation

Hamiltonian

$$\hat{H}_M = \begin{pmatrix} \hat{H}_0 & 0 & 0 \\ 0 & \hat{H}_{\mathrm{I}} & 0 \\ 0 & 0 & \hat{H}_{\mathrm{II}} \end{pmatrix} \qquad \boldsymbol{\mu} = \boldsymbol{\mu}^{\uparrow} + \boldsymbol{\mu}^{\downarrow} = \begin{pmatrix} 0 & \mu_{0,\mathrm{I}} & 0 \\ 0 & 0 & \mu_{\mathrm{I,II}} \\ 0 & 0 & 0 \end{pmatrix} + \begin{pmatrix} 0 & 0 & 0 \\ \mu_{\mathrm{I},0} & 0 & 0 \\ 0 & \mu_{\mathrm{II,I}} & 0 \end{pmatrix}$$

Doorway operators

$$\hat{D}_0(\omega_{pu}) = \int_{-\infty}^{\infty} dt_2' \int_0^{\infty} dt_1 E_{pu}(t_2') E_{pu}(t_2' - t_1) e^{i\omega_{pu}t_1} e^{-i\hat{H}_{\mathrm{I}}t_1} \mu_{\mathrm{I},0} \hat{\rho}_{0,0} e^{i\hat{H}_0 t_1} \mu_{0,\mathrm{I}} + \mathrm{h.c.}$$

$$\hat{D}_{\mathrm{I}}(\omega_{pu}) = \int_{-\infty}^{\infty} dt_2' \int_0^{\infty} dt_1 E_{pu}(t_2') E_{pu}(t_2' - t_1) e^{i\omega_{pu}t_1} \mu_{0,\mathrm{I}} e^{-i\hat{H}_{\mathrm{I}}t_1} \mu_{\mathrm{I},0} \hat{\rho}_{0,0} e^{i\hat{H}_0 t_1} + \mathrm{h.c.}$$

Window operators

$$\hat{W}_0(\omega_{pr}) = \int_{-\infty}^{\infty} dt' \int_0^{\infty} dt_3 E_{pr}(t') E_{pr}(t' + t_3) e^{i\omega_{pr}t_3} e^{i\hat{H}_0 t_3} \mu_{0,\mathrm{I}} e^{-i\hat{H}_{\mathrm{I}}t_3} \mu_{\mathrm{I},0} + \mathrm{h.c.}$$

$$\hat{W}_I(\omega_{pr}) = \int_{-\infty}^{\infty} dt' \int_0^{\infty} dt_3 E_{pr}(t') E_{pr}(t' + t_3) e^{i\omega_{pr}t_3} \mu_{\mathrm{I},0} e^{i\hat{H}_0 t_3} \mu_{0,\mathrm{I}} e^{-i\hat{H}_{\mathrm{I}}t_3} + \mathrm{h.c.}$$

$$\hat{W}_{\mathrm{II}}(\omega_{pr}) = \int_{-\infty}^{\infty} dt' \int_0^{\infty} dt_3 E_{pr}(t') E_{pr}(t' + t_3) e^{i\omega_{pr}t_3} \mu_{\mathrm{I,II}} e^{-i\hat{H}_{\mathrm{II}}t_3} \mu_{\mathrm{II,I}} e^{i\hat{H}_{\mathrm{I}}t_3} + \mathrm{h.c.}$$

(1) Gelin, M. F.; Huang, X.; Xie, W.; Chen, L.; Doslic, N. A.; Domcke, W. *J Chem Theory Comput* **2021,** *17*, 2394-2408.

(2) Mukamel, S. Principles of Nonlinear Optical Spectroscopy. **1995**.

Doorway-Window Approximations of Signals

the signal is defined as

$$S_{int}(\tau,\omega_{pr}) = S_{int}^{GSB}(\tau,\omega_{pr}) + S_{int}^{SE}(\tau,\omega_{pr}) + S_{int}^{ESA}(\tau,\omega_{pr})$$

$$S_{int}^{GSB}(\tau,\omega_{pr}) = \int d\boldsymbol{R}_g d\boldsymbol{P}_g \hat{D}_{0,IC}(\omega_{pu},\boldsymbol{R}_g,\boldsymbol{P}_g)\hat{W}_{0,IC}^{int}(\omega_{pr},\boldsymbol{R}_g(\tau),\boldsymbol{P}_g(\tau))$$

$$S_{int}^{SE}(\tau,\omega_{pr}) = \int d\boldsymbol{R}_g d\boldsymbol{P}_g \hat{D}_{\mathrm{I,IC}}(\omega_{pu},\boldsymbol{R}_e,\boldsymbol{P}_e)\hat{W}_{\mathrm{I,\,IC}}^{int}(\omega_{pr},\boldsymbol{R}_e(\tau),\boldsymbol{P}_e(\tau))$$

$$S_{int}^{ESA}(\tau,\omega_{pr}) = -\int d\boldsymbol{R}_g d\boldsymbol{P}_g \hat{D}_{\mathrm{I,IC}}(\omega_{pu},\boldsymbol{R}_e,\boldsymbol{P}_e)\hat{W}_{\mathrm{II,\,IC}}^{int}(\omega_{pr},\boldsymbol{R}_e(\tau),\boldsymbol{P}_e(\tau))$$

Doorway-Window Approximations of Signals

If we allow internal conversion

$$D_{0,IC}(\omega_{pu}, \boldsymbol{R}_g, \boldsymbol{P}_g) = \begin{cases} D_0(\omega_{pu}, \boldsymbol{R}_g, \boldsymbol{P}_g), \text{if trajectory stays within } \{0\} \\ 0, \text{if trajectory stays within } \{\mathrm{I}\} \\ -D_I(\omega_{pu}, \boldsymbol{R}_g, \boldsymbol{P}_g), \text{if trajectory jumps from } \{\mathrm{I}\} \text{ to } \{0\} \end{cases}$$

$$D_{I,IC}(\omega_{pu}, \boldsymbol{R}_e, \boldsymbol{P}_e) = \begin{cases} 0, \text{if trajectory stays within } \{0\} \\ D_I(\omega_{pu}, \boldsymbol{R}_e, \boldsymbol{P}_e), \text{if trajectory stays within } \{\mathrm{I}\} \\ 0, \text{if trajectory jumps from } \{\mathrm{I}\} \text{ to } \{0\} \end{cases}$$

Doorway-Window Approximations of Signals

and

$$W_{0,IC}^{int}(\omega_{pr}, \boldsymbol{R}_g(\tau), \boldsymbol{P}_g(\tau)) = \begin{cases} W_0^{int}(\omega_{pr}, \boldsymbol{R}_g(\tau), \boldsymbol{P}_g(\tau)), & \text{if trajectory stays within } \{0\} \\ 0, & \text{if trajectory stays within } \{\mathrm{I}\} \\ W_0^{int}(\omega_{pr}, \boldsymbol{R}_g(\tau), \boldsymbol{P}_g(\tau)), & \text{if trajectory jumps from } \{\mathrm{I}\} \text{ to } \{0\} \end{cases}$$

$$W_{I,IC}^{int}(\omega_{pr}, \boldsymbol{R}_e(\tau), \boldsymbol{P}_e(\tau)) = \begin{cases} 0, & \text{if trajectory stays within } \{0\} \\ W_I^{int}(\omega_{pr}, \boldsymbol{R}_e(\tau), \boldsymbol{P}_e(\tau)), & \text{if trajectory stays within } \{\mathrm{I}\} \\ 0, & \text{if trajectory jumps from } \{\mathrm{I}\} \text{ to } \{0\} \end{cases}$$

$$W_{II,IC}^{int}(\omega_{pr}, \boldsymbol{R}_e(\tau), \boldsymbol{P}_e(\tau)) = \begin{cases} 0, & \text{if trajectory stays within } \{0\} \\ W_{II}^{int}(\omega_{pr}, \boldsymbol{R}_e(\tau), \boldsymbol{P}_e(\tau)), & \text{if trajectory stays within } \{\mathrm{I}\} \\ 0, & \text{if trajectory jumps from } \{\mathrm{I}\} \text{ to } \{0\} \end{cases}$$

Photoinduced Energy Transfers in Dendrimers

Nanostar dendrimer

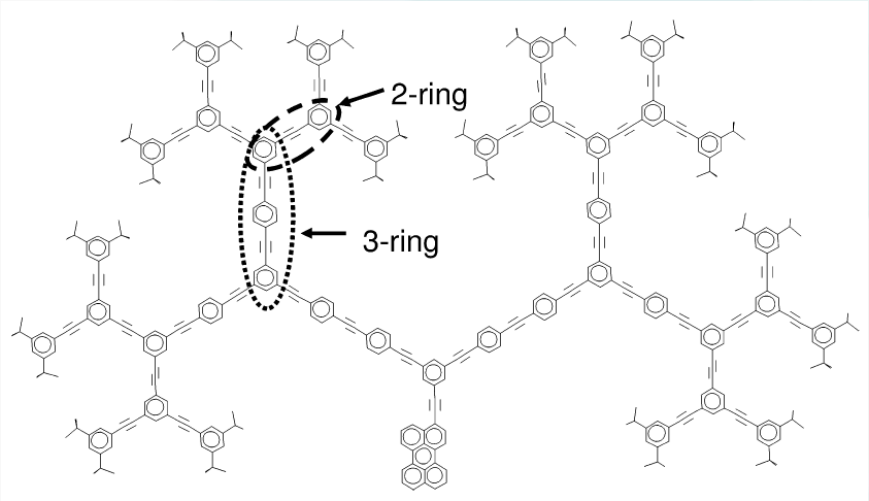

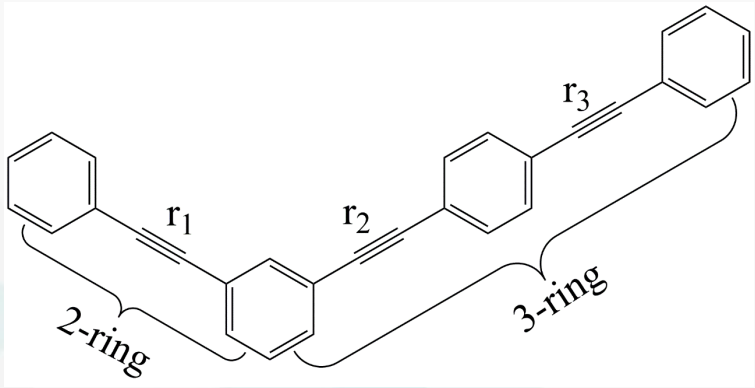

- Photoinduced energy transfer process occurs from the short-length to the long-length units in dendrimer system ultrafastly.

(1) Kirkwood, J. C.; Scheurer, C.; Chernyak, V.; Mukamel, S. *J. Chem. Phys.* **2001,** *114*, 2419-2429.
(2) Kleiman, V. D.; Melinger, J. S.; McMorrow, D. *J. Phys. Chem. B* **2001,** *105*, 5595-5598.
(3) Ortiz, W.; Krueger, B. P.; Kleiman, V. D.; Krause, J. L.; Roitberg, A. E. *J. Phys. Chem. B* **2005,** *109*, 11512-9.
(4) Huang, J.; Du, L.; Hu, D.; Lan, Z. *J Comput Chem* **2015,** *36*, 151-63.
(5) Nelson, T.; Fernandez-Alberti, S.; Roitberg, A. E.; Tretiak, S. *Acc. Chem. Res.* **2014,** *47*, 1155-1164
(6) Freixas, V. M.; Ondarse-Alvarez, D.; Tretiak, S.; Makhov, D. V.; Shalashilin, D. V.; Fernandez-Alberti, S. *J. Chem. Phys.* **2019,** *150*, 124301.

Excited States of Dendrimers

Electronic structure calculations (TD/CAM-B3LYP/6-31G)

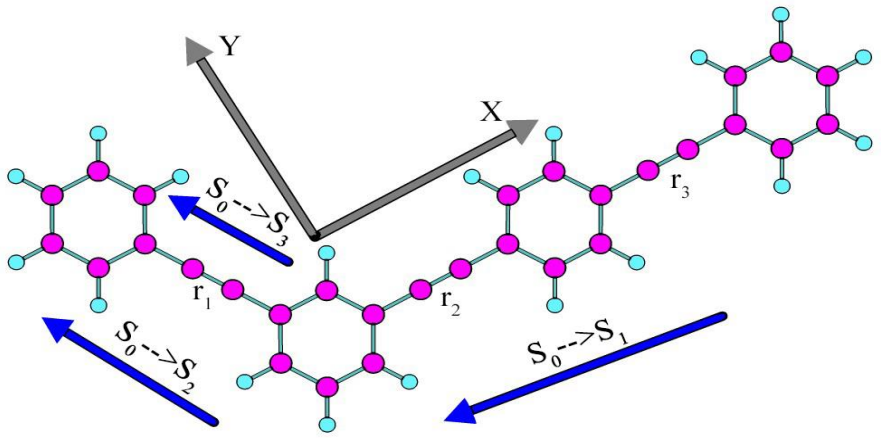

	VEE (eV)	TDM (Debye)			Dominant Contributions
		X	Y	Z	
S_1	4.03	12.09	-1.36	0	HOMO → LUMO 82.5%
S_2	4.64	2.88	-5.97	0	HOMO-1 → LUMO+1 58.9% HOMO-1 → LUMO 21.1%
S_3	4.71	0.77	-1.41	0	HOMO → LUMO+1 28.4% HOMO-1 → LUMO 17.5% HOMO-1 → LUMO+2 11.4 %
S_4	4.99	0	-0.09	0	HOMO → LUMO+3 43.0% HOMO-5 → LUMO 41.5%

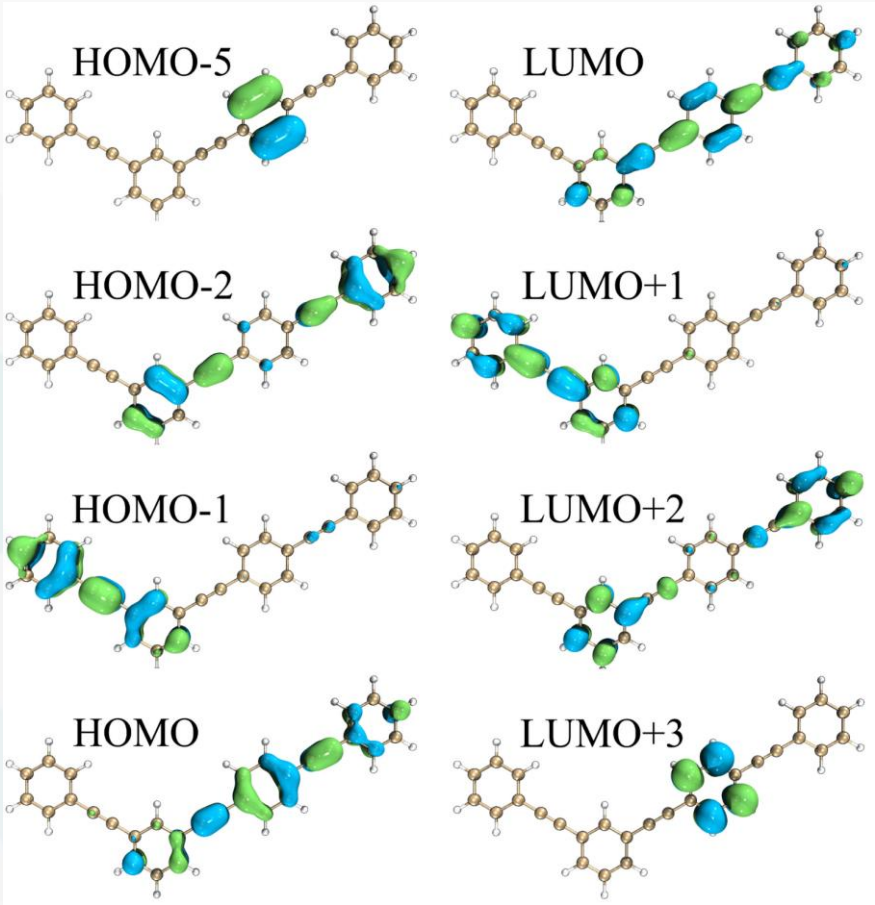

- S_1 is nearly a LE state at the 3-ring unit
- S_2 is a hybrid LE state at the 2-ring unit and CT state.

On-the-Fly BOMD and Nonadiabatic Dynamics

Nonadiabatic dynamics

- Fewest switches trajectories surface hopping
- Nonadiabatic dynamics start from S_1, S_2, and S_3 with 200 trajectories
- BO dynamics at ground state
- Transition dipole moment between excited states (up to 150) are recorded

Time-dependent electronic populations

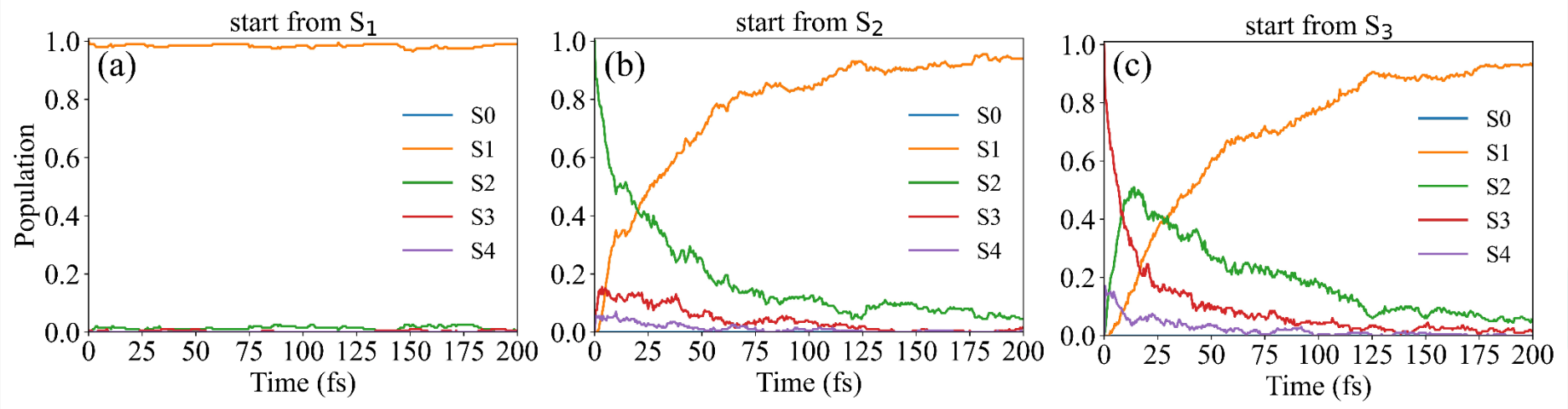

- The electronic population decays to S1 very efficiently from high-lying excited states.

Transient-Absorption Pump-Probe Integral Signals

$\omega_{pu} = 4.03\ eV$ resonant with S_1

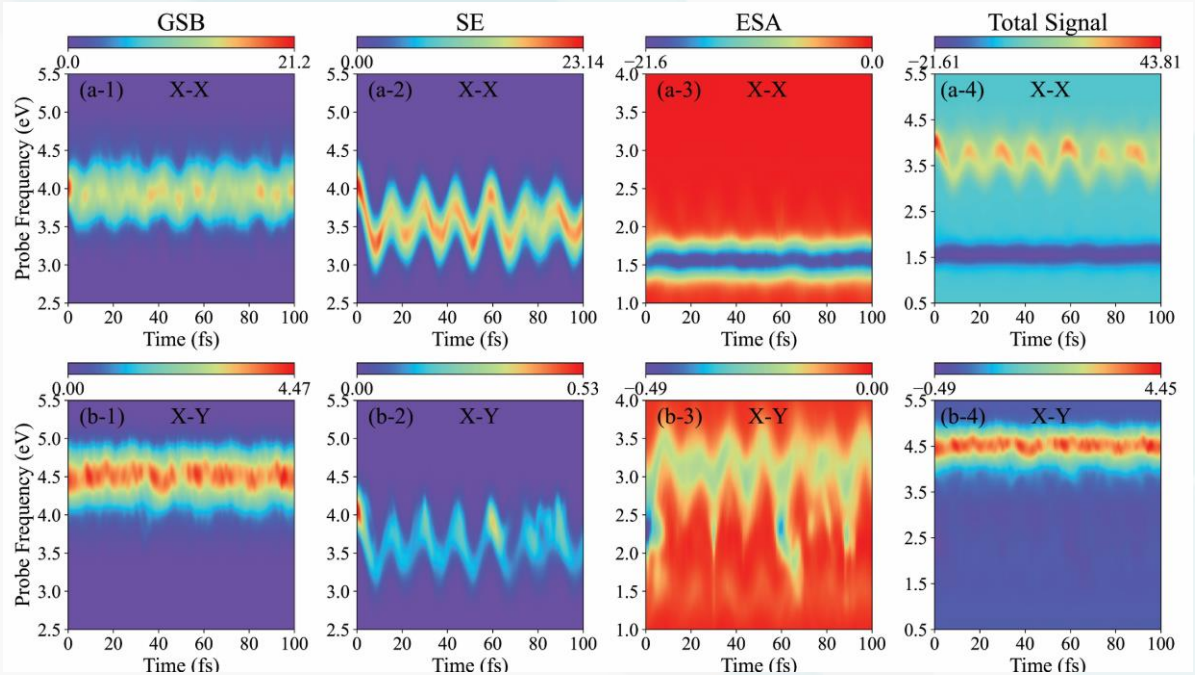

Pump X probe X

Pump X probe Y

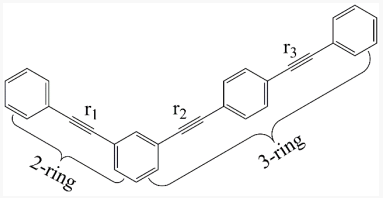

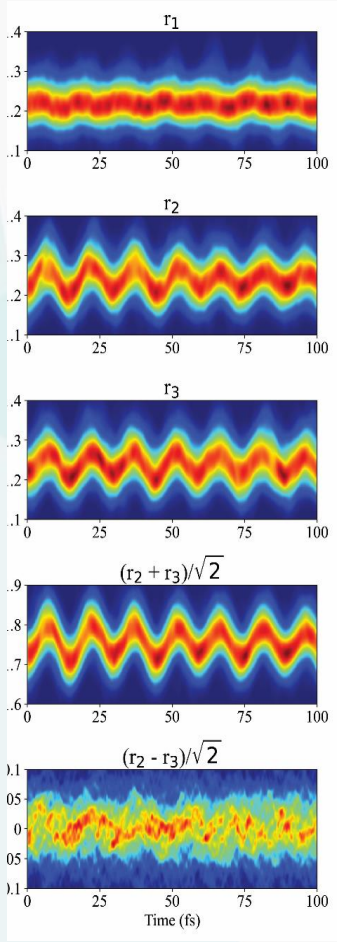

- The oscillation of the SE signal is induced by the symmetric stretching vibration of the CC triplet bonds (r2 and r3) at the 3-ring unit.

Hu, Peng, Chen, Gelin, Lan, *JPCL,* 2021, 12, 39, 9710–9719

Transient-Absorption Pump-Probe Integral Signals

$\omega_{pu} = 4.64\ eV$ *resonant with* S_2

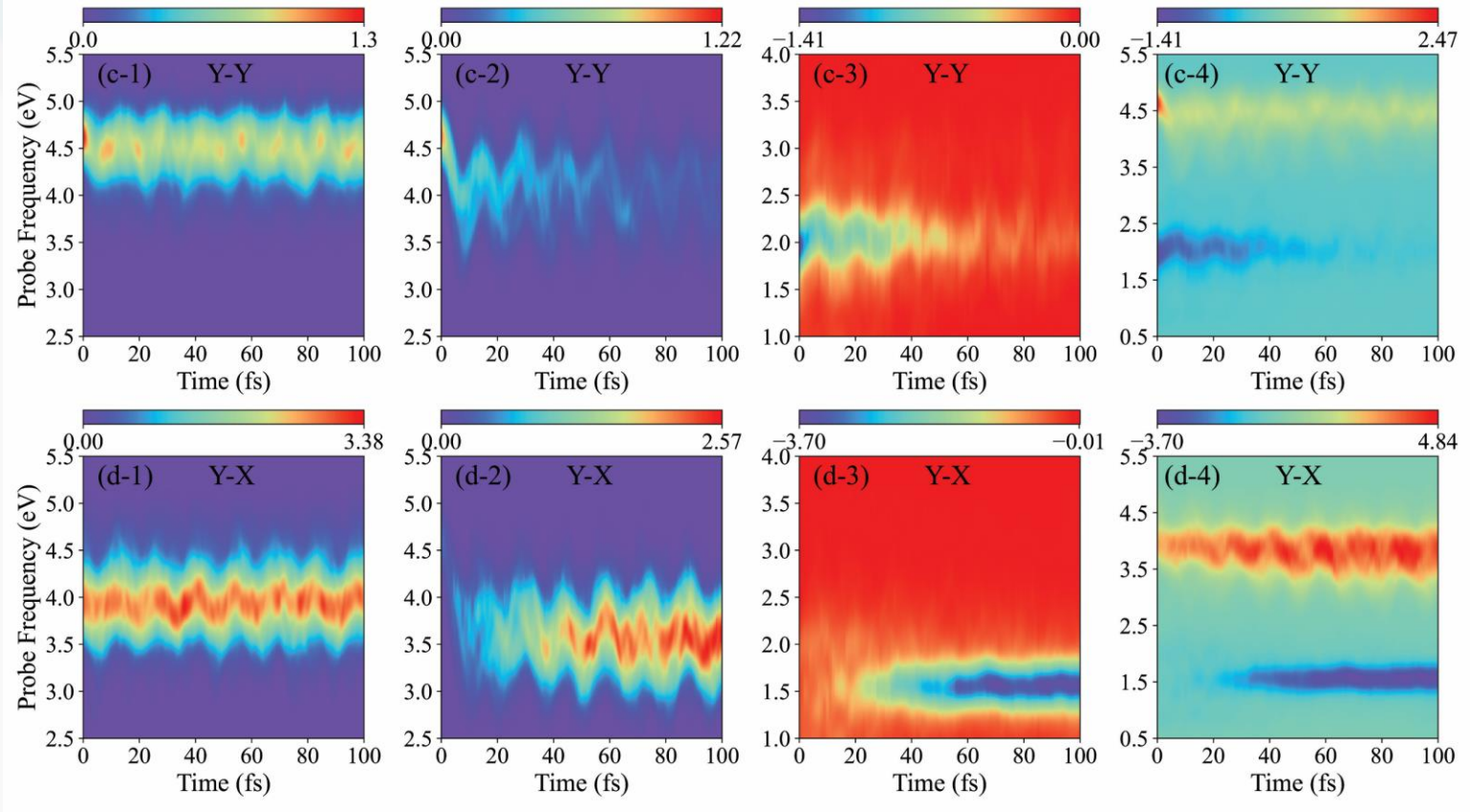

- The disappearance of the signal in the Y-axis direction and appearance in the X-axis direction clearly indicates the energy transfer process from the 2-ring to 3-ring unit.

Hu, Peng, Chen, Gelin, Lan, *JPCL,* 2021, 12, 39, 9710–9719

Transient-Absorption Pump-Probe Dispersed Signals

$\omega_{pu} = 4.03\ eV$ resonant with S_1

Pump Y
probe Y

Pump Y
probe X

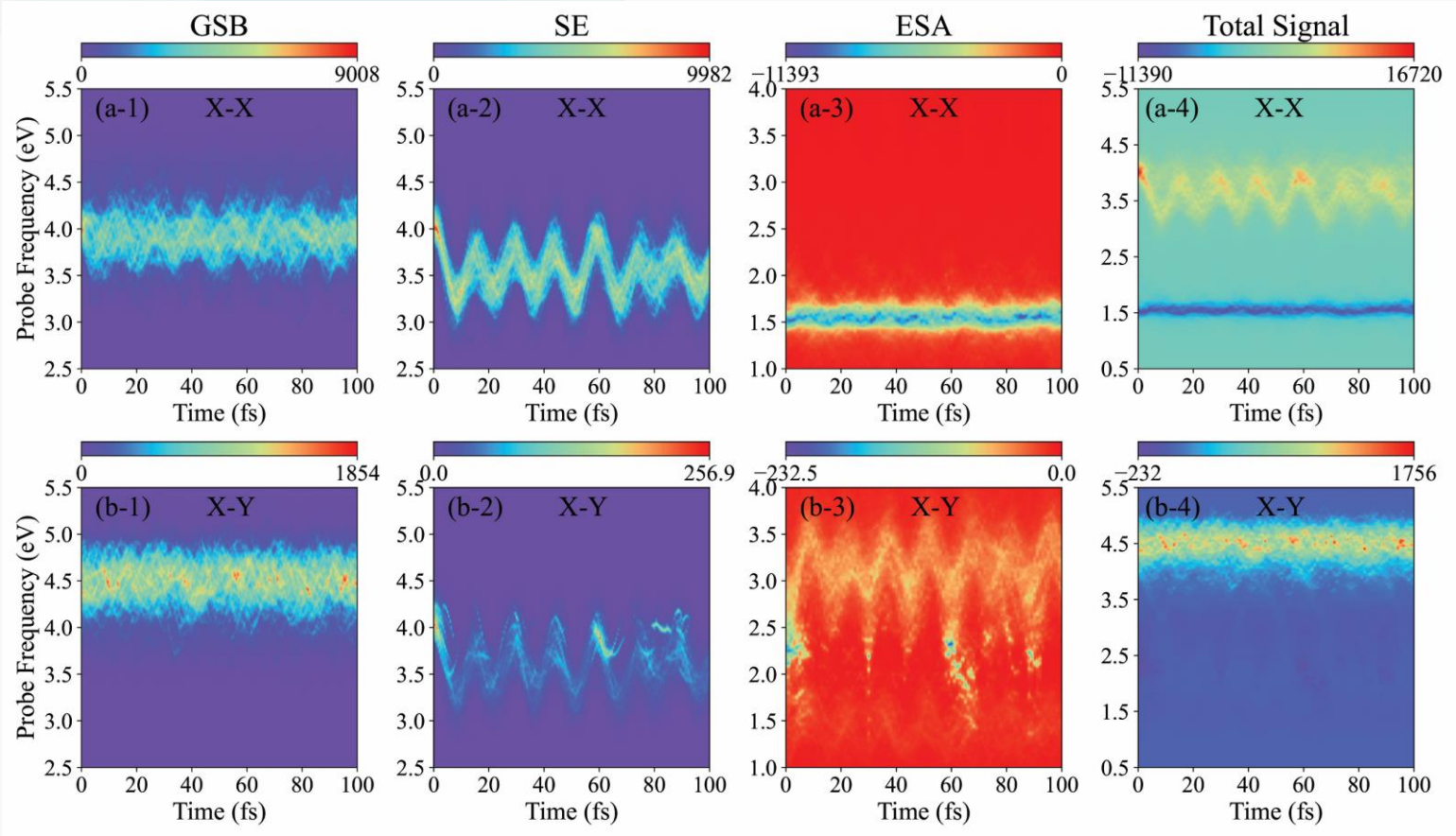

Hu, Peng, Chen, Gelin, Lan, *JPCL,* 2021, 12, 39, 9710–9719

Transient-Absorption Pump-Probe Dispersed Signals

$\omega_{pu} = 4.64\ eV$ *resonant with* S_2

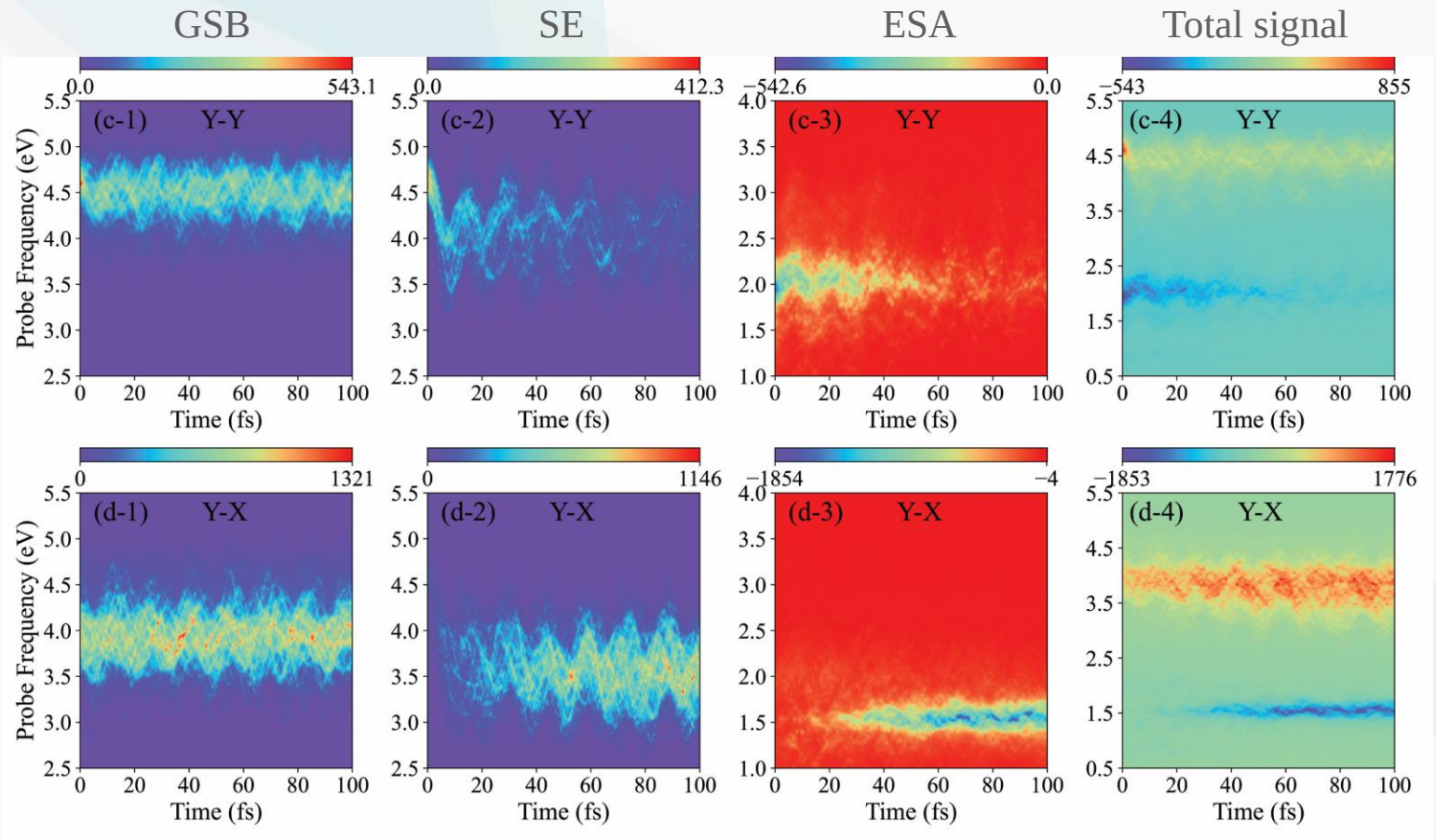

Hu, Peng, Chen, Gelin, Lan, *JPCL,* 2021, 12, 39, 9710–9719

Message to take home

- The polarizable TA PP signals are useful tool to detect the excited-state energy transfer processes, if the involved excited states display different transition energies, transition-dipole-moment orientations.

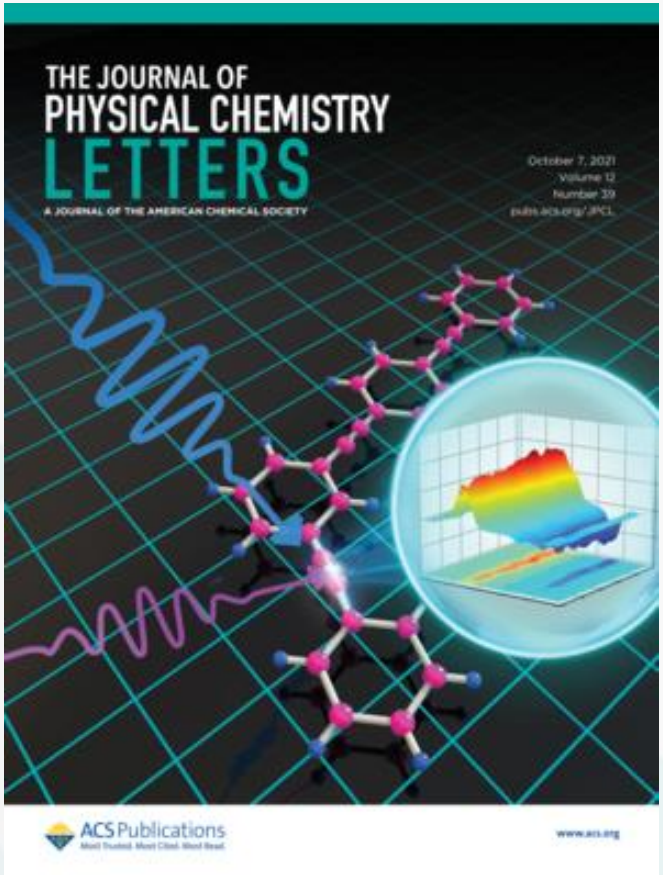

Hu, Peng, Chen, Gelin, Lan, *JPCL,* 2021, 12, 39, 9710–9719

Nonadiabatic Dynamics of Azomethane ($CH_3N=NCH_3$)

Nonadiabatic dynamics

- Fewest switches trajectories surface hopping
- Nonadiabatic dynamics start from S_1 with 200 trajectories
- BO dynamics at ground state to calculate GSB signals
- Transition dipole moment between excited states are recorded

Electronic structure calculations

- OM2/MRCI(8, 7) by MNDO
- SA-CASSCF(6, 4)/6-31G* by Molpro
- XMS-CASPT2(6, 4)/cc-pVDZ by BAGEL

  Interface to JADE

DOI: 10.1021/acs.jpclett.1c03373

the nonadiabatic dynamics of azomethane

Time-dependent electronic populations

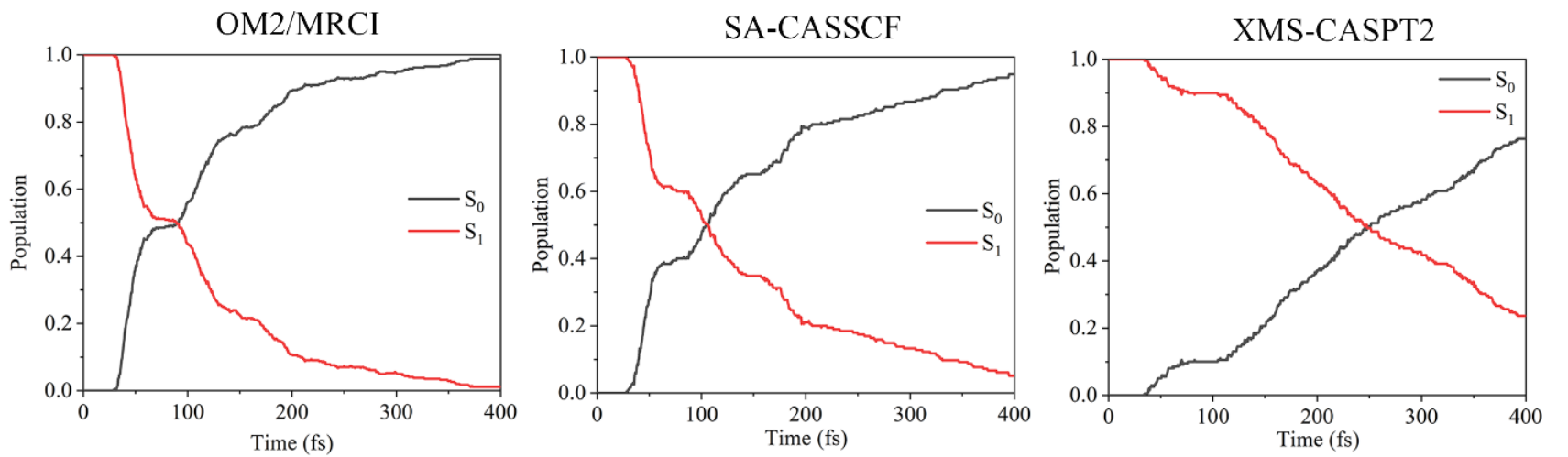

- Similar population dynamics are obtained in the TSH dynamics at the OM2/MRCI and SA-CASSCF levels
- The TSH dynamics at the XMS-CASPT2 level shows a longer time scale (249 fs)

DOI: 10.1021/acs.jpclett.1c03373

Integral TA PP signal of azomethane

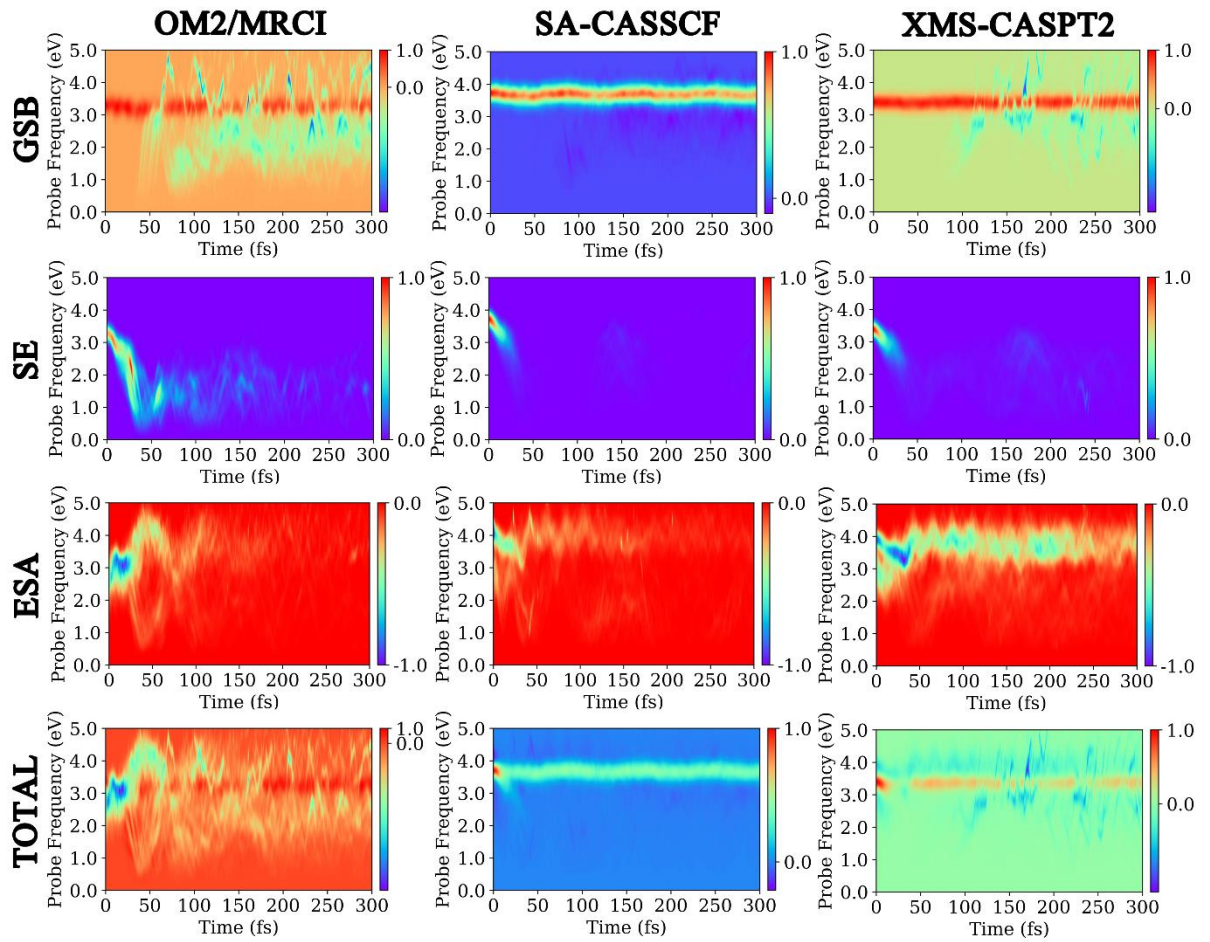

- OM2/MRCI signal is initially dominated by ESA, but later exhibits hot and cold GSB
- SA-CASSCF signal is dominated by the cold GSB
- XMS-CASPT2 signals exhibits pronounced GSB and ESA

- The early-time TA PP signals in the SA-CASSCF and XMS-CASPT2 spectra are similar, which correspond to SE.

DOI: 10.1021/acs.jpclett.1c03373

Non-Condon Effects

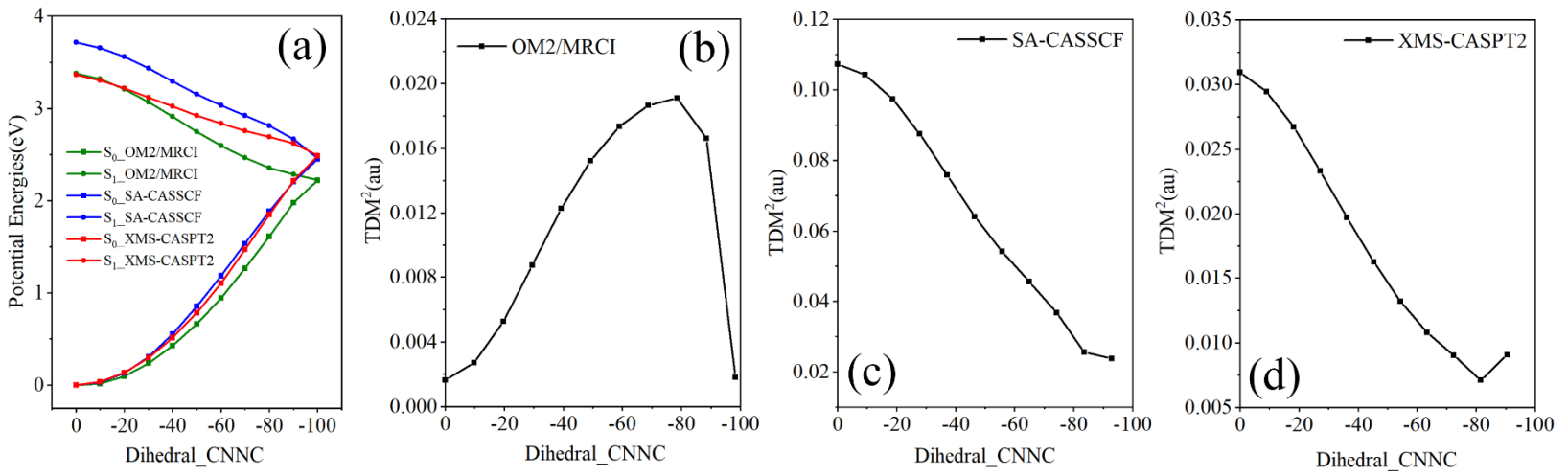

- XMS-CASPT2 pathway is flatter compared to the OM2/MRCI and SA-CASSCF pathways.
- The S_0-S_1 TDMs depend dramatically on the chosen levels of the electronic structure theories.
- Non-Condon effect is important in the explanation of TA PP signals.

Message to Take Home

- Nonadiabatic population dynamics and time-resolved stimulated-emission signals may not contain identical information, owing to the non-Condon effects.
- Different electronic-structure methods may have different impacts on simulated population dynamics and time-resolved TA PP spectra.

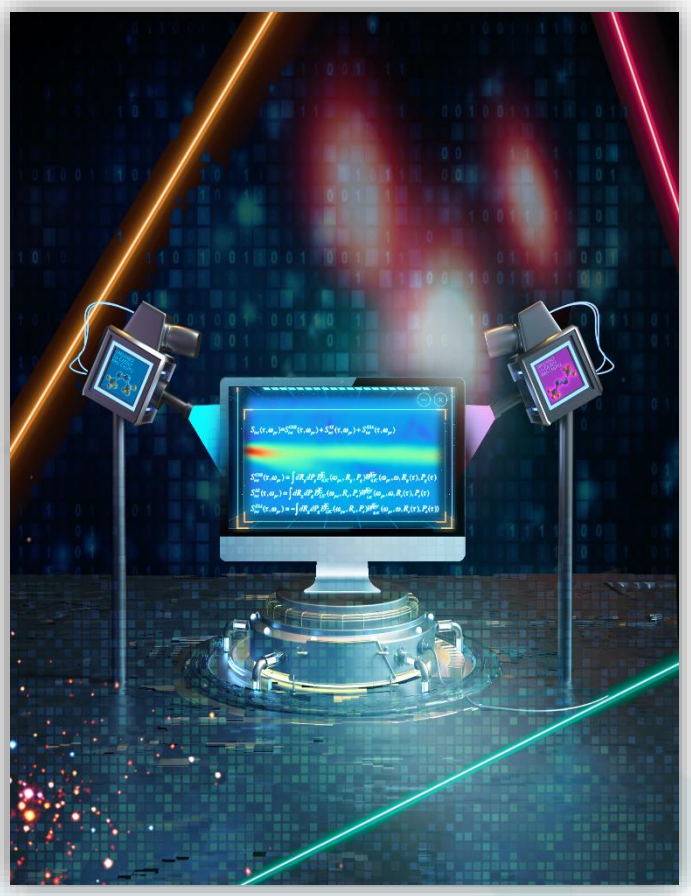

DOI: 10.1021/acs.jpclett.1c03373

Excited-State Dynamics

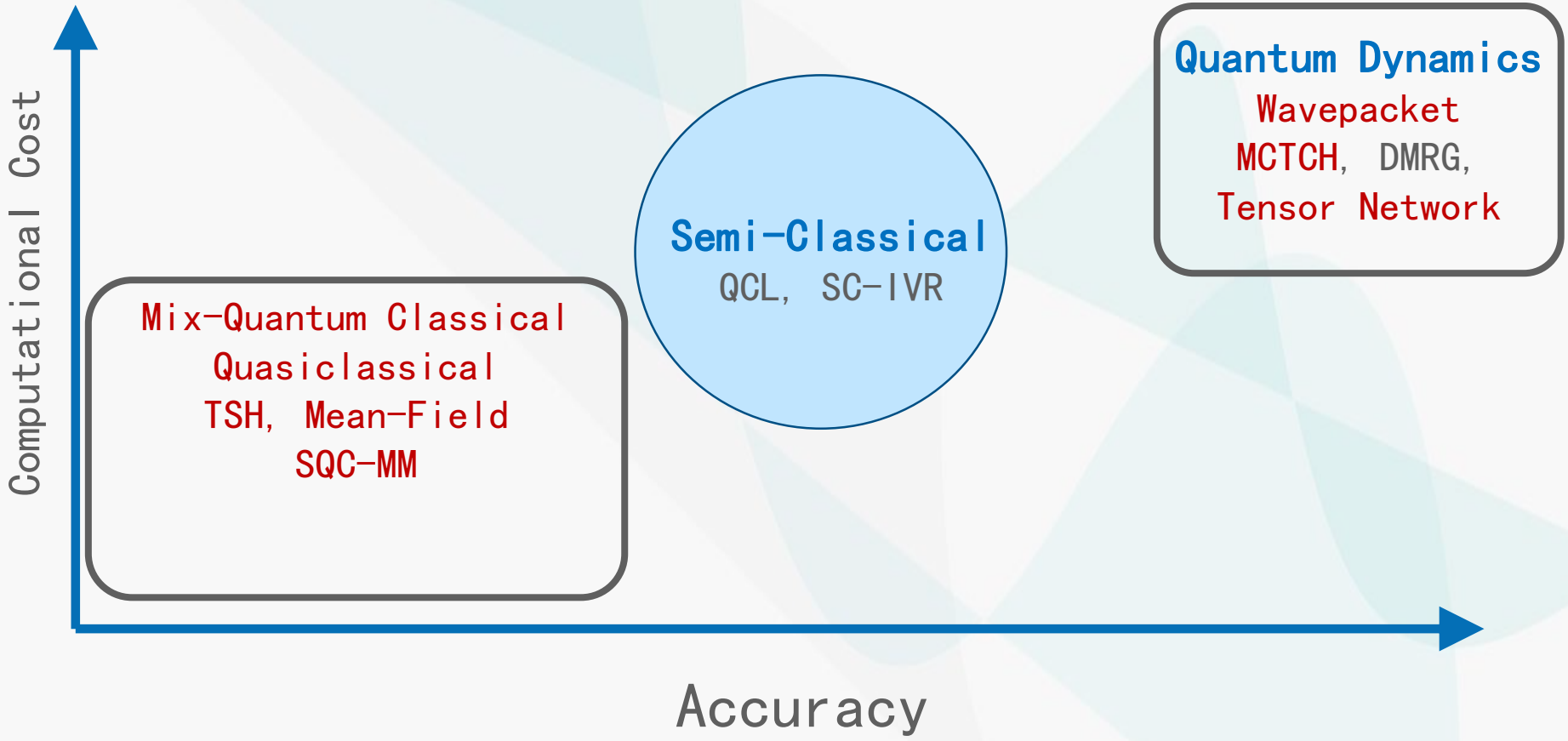

ML-MCTDH

Standard propagation method (f_{max}~ 10)

$$\Psi\left(Q_1,\cdots,Q_f,t\right)=\sum_{j_1=1}^{N_1}\cdots\sum_{j_f=1}^{N_f}C_{j_1\cdots j_f}\left(t\right)\prod_{\kappa=1}^{f}\chi_{j_\kappa}^{(\kappa)}\left(Q_\kappa\right)$$

$$i\frac{\partial}{\partial t}C_J=\sum_L H_{JL}C_L$$

MCTDH (f_{max}~ 60)

$$\Psi\left(Q_1,\cdots,Q_f,t\right)=\sum_{j_1=1}^{n_1}\cdots\sum_{j_f=1}^{n_f}A_{j_1\cdots j_f}\left(t\right)\prod_{\kappa=1}^{f}\varphi_{j_\kappa}^{(\kappa)}\left(Q_\kappa,t\right)$$

$$i\dot{A}_J=\sum_L\left\langle\Phi_J\left|H\right|\Phi_L\right\rangle A_L$$

$$i\dot{\boldsymbol{\varphi}}^{(\kappa)}=\left(1-P^{(\kappa)}\right)\left(\boldsymbol{\rho}^{(\kappa)}\right)^{-1}\left\langle H\right\rangle^{(\kappa)}\boldsymbol{\varphi}^{(\kappa)}$$

ML-MCTDH (f_{max}~ 1500)

$$\varphi_m^{z-1,}\left(Q_{\kappa_{l-1}}^{z-1},t\right)=\sum_{j_1=1}^{n_1}\cdots\sum_{j_{p_{\kappa_l}}=1}^{n_{\kappa_l}}A_{j_1\cdots j_{p_{\kappa_l}}}^{z}\left(t\right)\prod_{\kappa_l=1}^{p_{\kappa_l}}\varphi_{j_{\kappa_l}}^{z,\kappa_l}\left(Q_{\kappa_l}^{z},t\right)$$

$$i\dot{A}_J^l=\sum_L\left\langle\Phi_J^l\left|H\right|\Phi_L^l\right\rangle A_L^l$$

$$i\dot{\varphi}_n^{z,\kappa_l}=\left(1-\hat{P}_{\kappa_l}^{z}\right)\sum\left(\rho^{z,\kappa_l}\right)_{nj}^{-1}\left\langle H\right\rangle_{jm}^{z,\kappa_l}\varphi_m^{z,\kappa_l}$$

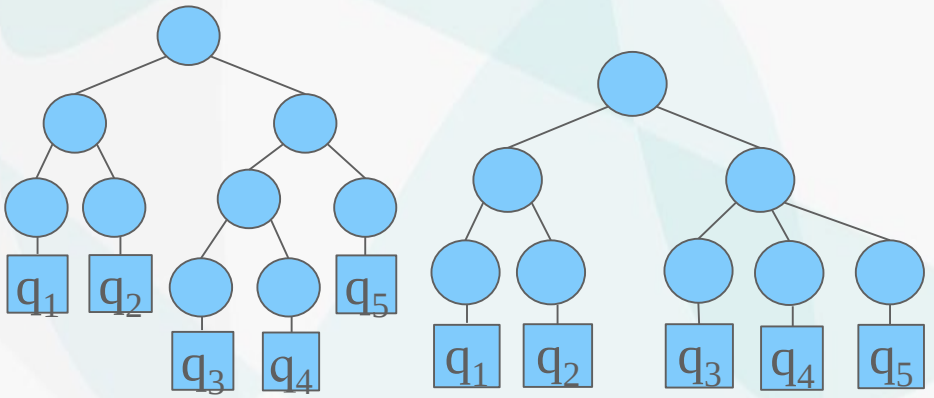

Transfer-Tensor Method

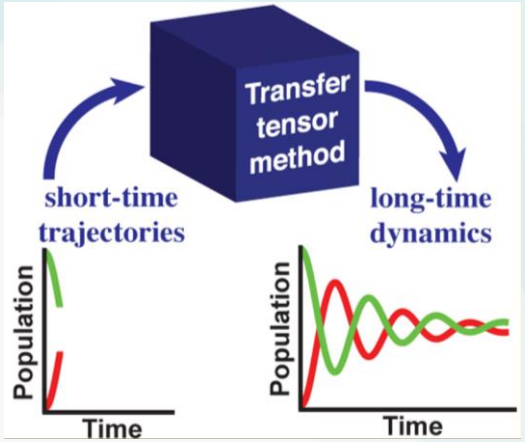

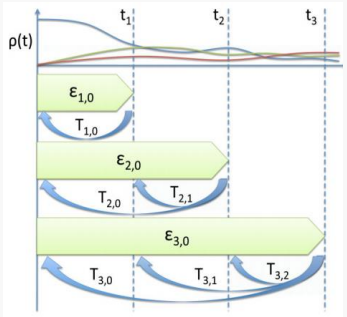

$$T_{n,0} = \mathcal{E}_n - \sum_{m=1}^{n-1} T_{n,m}\mathcal{E}_m,$$

$$\rho(t_n) = \sum_{k=0}^{n-1} T_{n,k}\rho(t_k)$$

$$\rho(t_m) = (T_1 T_2 \ldots T_K) \begin{pmatrix} \rho(t_{m-1}) \\ \rho(t_{m-2}) \\ \vdots \\ \rho(t_{m-K}) \end{pmatrix}$$

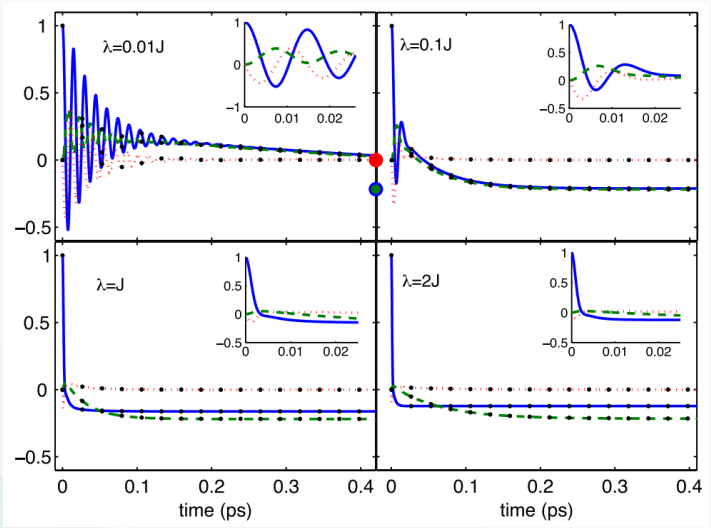

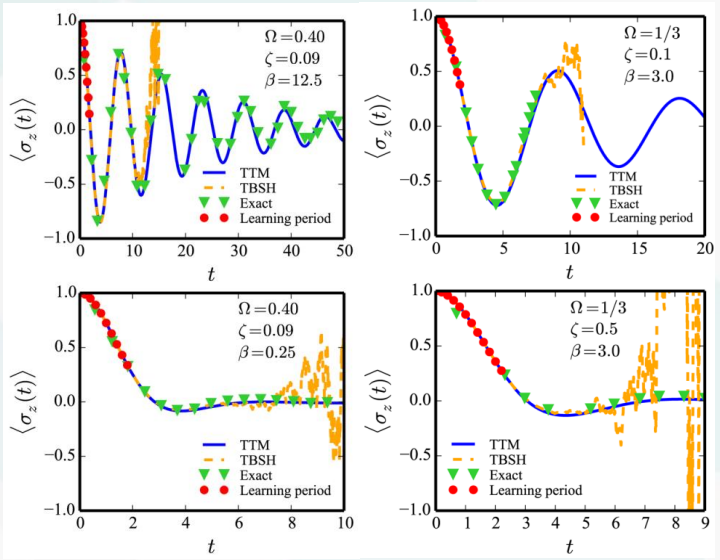

[Cerrillo, J.; Cao, J. ***Phy. Rev. Lett.***, 112, 110401 (2014)]

[Kananenka, A. A.; Hsieh, C.-Y.; Cao, J.; Geva, E. ***J. Phys. Chem. Lett.***, 7, 4809-4814 (2016)]

Long-Time Dynamics by ML Method

- **Artificial Neural Networks**

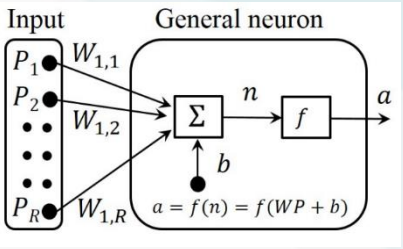

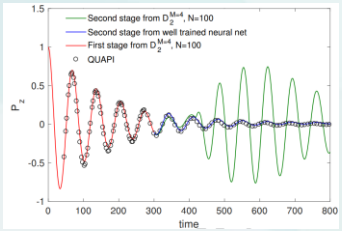

- **Kernel Ridge Regression**

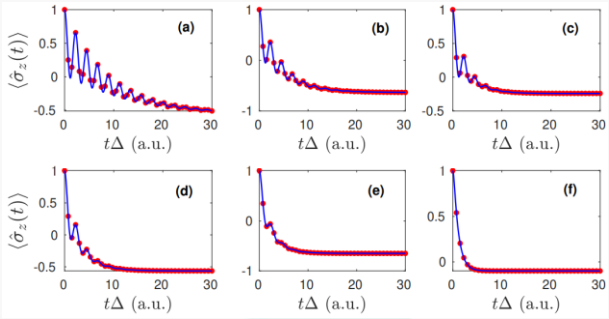

- **Recurrent Neural Networks**

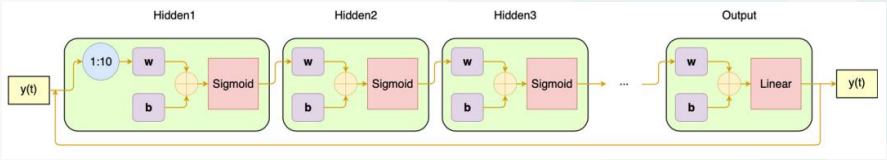

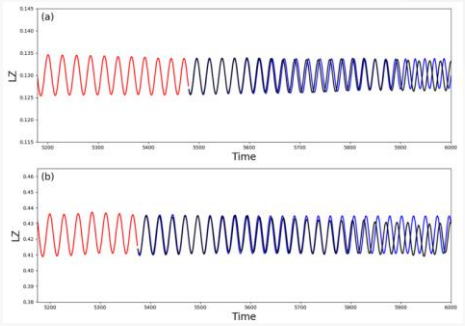

- **Convolutional Neural Networks**

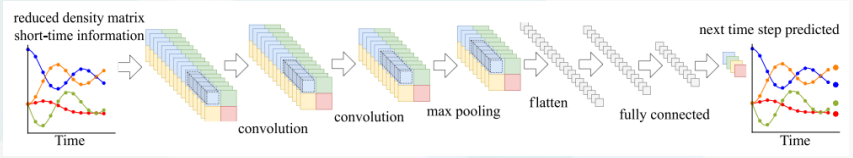

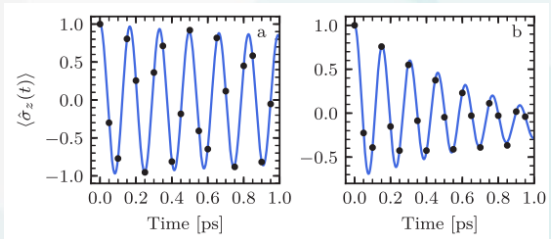

- Bandyopadhyay, S.; Huang, Z.; Sun, K.; Zhao, Y. ***Chem. Phys.,*** 515, 272-278 (2018)
- Yang, B.; He, B.; Wan, J.; Kubal, S.; Zhao, Y. ***Chem. Phys.,*** 528, 110509 (2020)
- Rodríguez, L. E. H.; Kananenka, A. A. ***J. Phys.*** Chem. Lett., 12, 2476-2483 (2021)
- Ullah, A; Dral, P. O, ***New J. Phys***., 2021, 23, 113019. DOI: 10.1088/1367-2630/ac3261.

Long Short-Term Memory RNN

- The Simple RNN

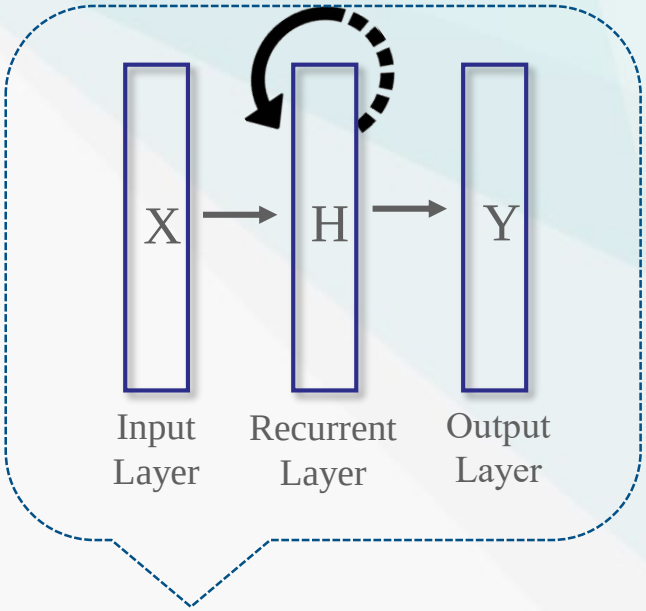

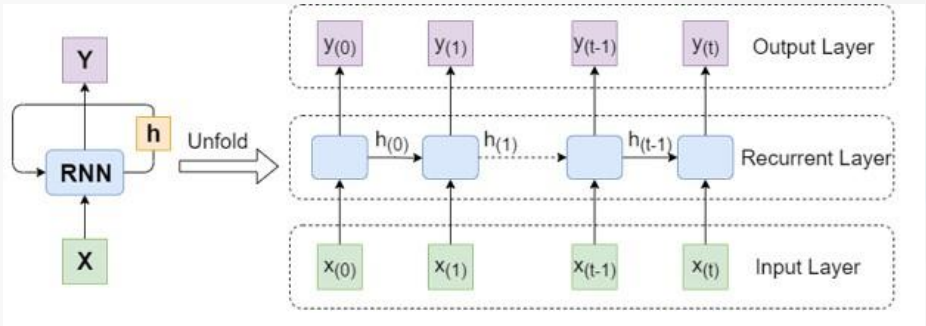

- The LSTM Cell

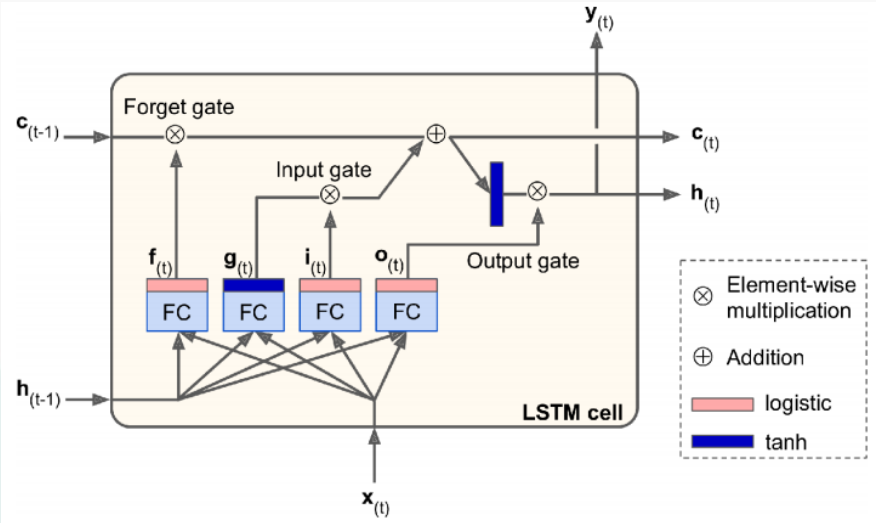

$$i_{(t)} = \sigma\left(W_{xi}^T x_{(t)} + W_{hi}^T h_{(t-1)} + b_i\right),$$

$$f_{(t)} = \sigma\left(W_{xf}^T x_{(t)} + W_{hf}^T h_{(t-1)} + b_f\right),$$

$$o_{(t)} = \sigma\left(W_{xo}^T x_{(t)} + W_{ho}^T h_{(t-1)} + b_o\right),$$

$$g_{(t)} = tanh\left(W_{xg}^T x_{(t)} + W_{hg}^T h_{(t-1)} + b_g\right),$$

$$c_{(t)} = f_{(t)} \cdot c_{(t-1)} + i_{(t)} \cdot g_{(t)},$$

$$y_{(t)} = h_{(t)} = o_{(t)} \cdot tanh\left(c_{(t)}\right).$$

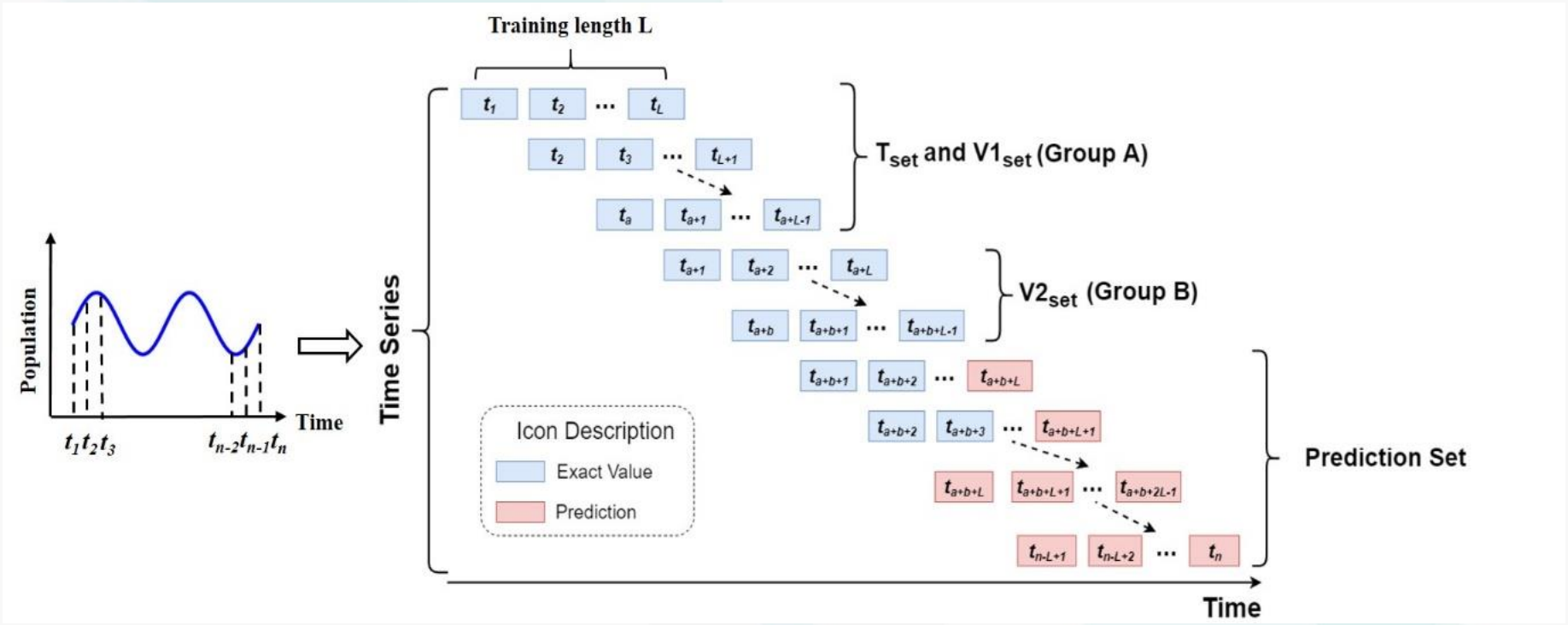
Training length L
Population
Time
$t_1 t_2 t_3$
$t_{n-2} t_{n-1} t_n$
Time Series
t_1 t_2 ... t_L
t_2 t_3 ... t_{L+1}
t_a t_{a+1} ... t_{a+L-1}
T_{set} and $V1_{set}$ (Group A)
t_{a+1} t_{a+2} ... t_{a+L}
t_{a+b} t_{a+b+1} ... $t_{a+b+L-1}$
$V2_{set}$ (Group B)
t_{a+b+1} t_{a+b+2} ... t_{a+b+L}
t_{a+b+2} t_{a+b+3} ... $t_{a+b+L+1}$
t_{a+b+L} $t_{a+b+L+1}$ ... $t_{a+b+2L-1}$
t_{n-L+1} t_{n-L+2} ... t_n
Prediction Set
Icon Description
Exact Value
Prediction
Time

Bootstrap Resampling Method

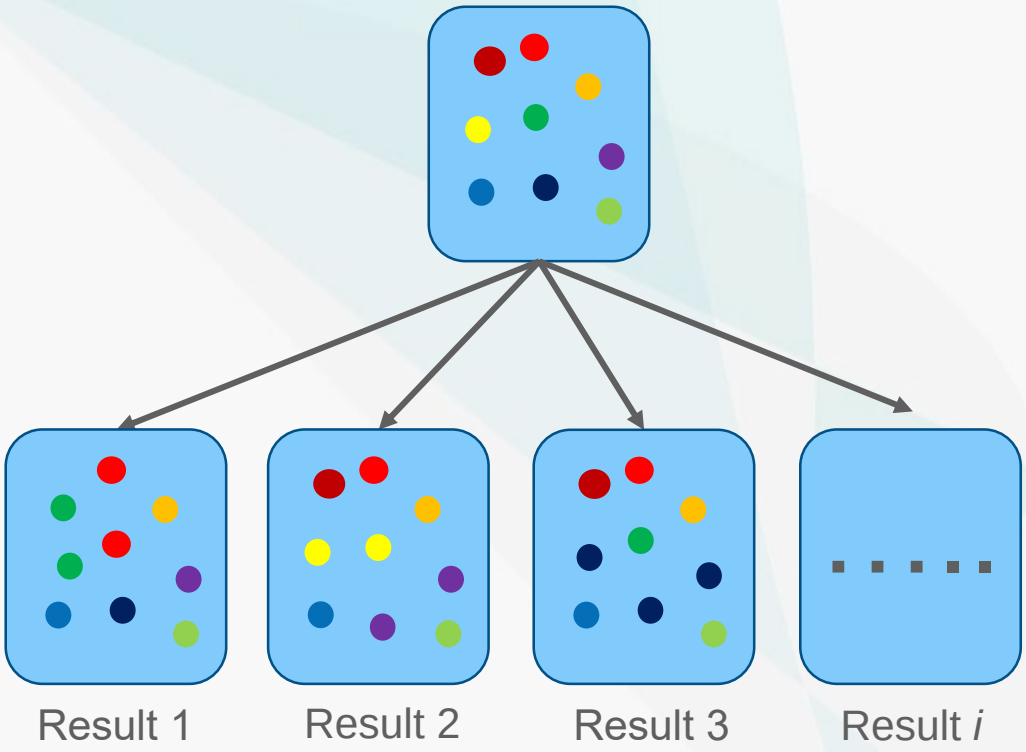

Bootstrap Distribution

$$X = [x_1, x_2, x_3, x_4, x_5, x_6, x_7, x_8]$$

bootstrap

$$X_1 = [x_1, x_3, x_3, x_2, x_2, x_2, x_7, x_8]$$

$$X_2 = [x_4, x_5, x_7, x_1, x_1, x_8, x_7, x_8]$$

$$X_3 = [x_6, x_2, x_4, x_4, x_5, x_7, x_7, x_8]$$

$$X_4 = [x_3, x_2, x_4, x_4, x_1, x_6, x_7, x_8]$$

……

- This powerful approach solves the model uncertainty and the model misspecification problems.

Simulation of Open Quantum Dynamics with Bootstrap-Based LSTM-NN

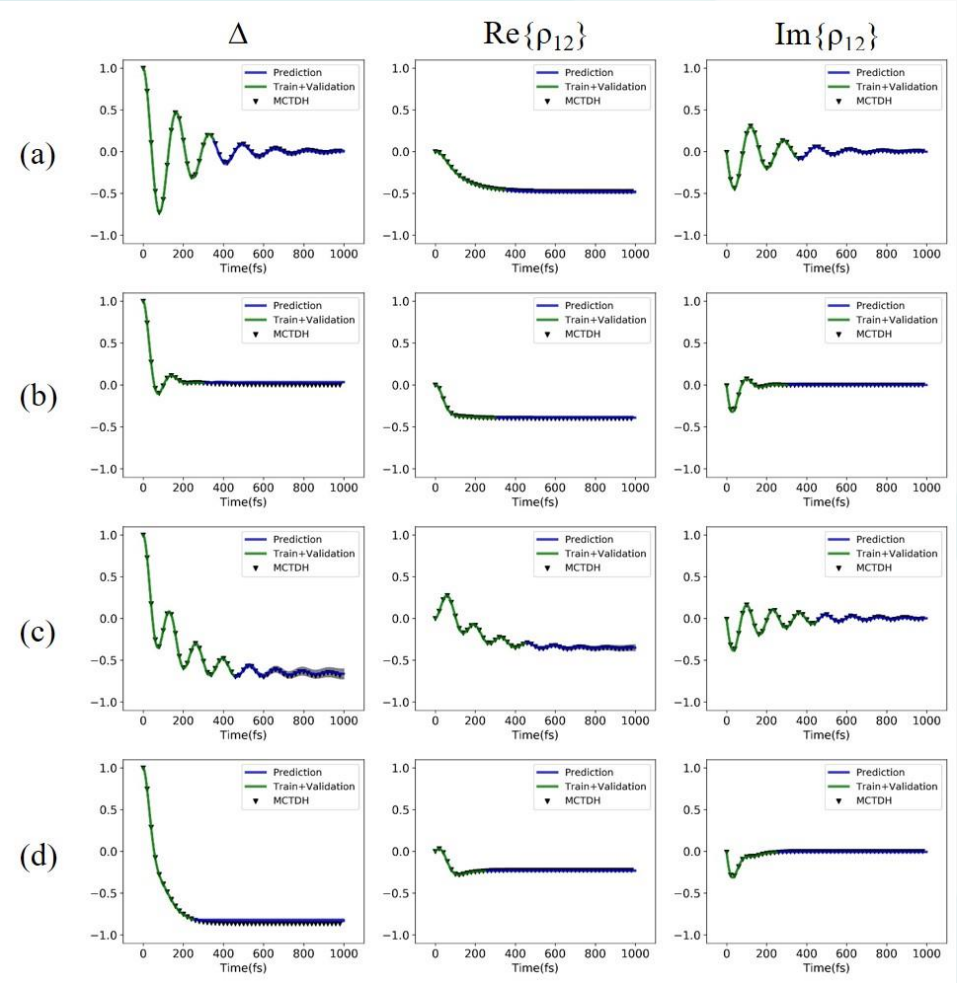

The quantum dynamics predicted by the bootstrap-based LSTM-NNs *vs.* the ML-MCTDH quantum dynamics with symmetric models of (a) and (b), asymmetric models of (c) and (d).

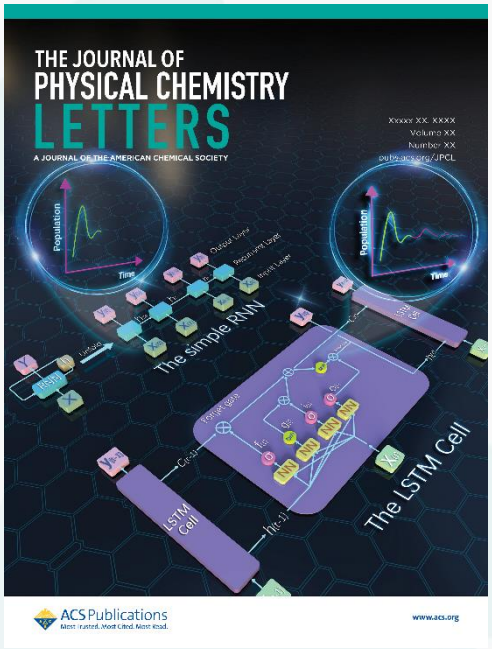

Lin, Peng, Gu, Lan, ***JPCL***. 10.1021/acs.jpclett.1c02672

Message to Take Home

- The LSTM-RNN models can be used to simulate the long-time dynamics evolutions of open quantum systems.
- The bootstrap resample method can give us the rough estimation of model uncertainty.

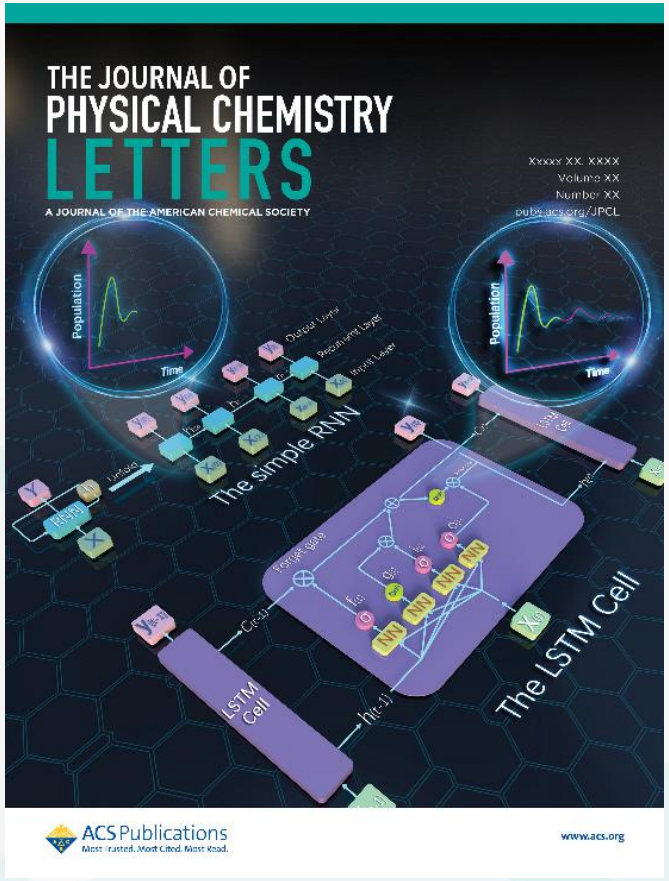

Lin, Peng, Gu, Lan, ***JPCL***. 10.1021/acs.jpclett.1c02672

Research highlights

Potential Energy Surfaces

Diabatization

Mixed quantum classical
Quasiclassical
Semiclassical
Dynamics

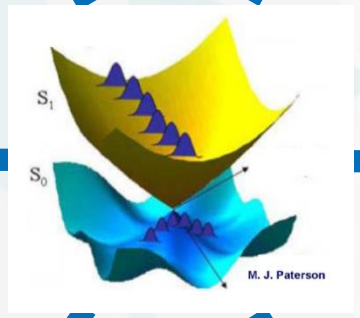

Quantum Wavepacket and Dissipative Dynamics

Machine Learning

Time-resolved spectroscopy

On-the-fly TSH Dynamics

Method and code developments:

Ab initio semiclassical nonadiabatic dynamics

- Initial sampling
- Surface-hopping dynamics (Tully, Zhu-Nakamura)
- Electronic structures: TDDFT, CIS, ADC(2), CASSCF
- Packages :Turbomole, Gaussian, GAMESS, Molpro
- All atoms; real systems; real time
- Analytical and numerical NAC

JADE

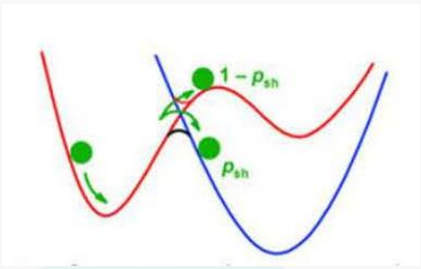

- On-the-fly TSH Dynamics
- Black-Box Simulation Tool
- Photo induced reactions

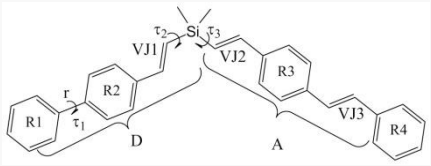

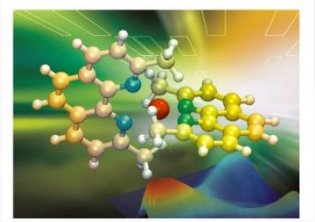

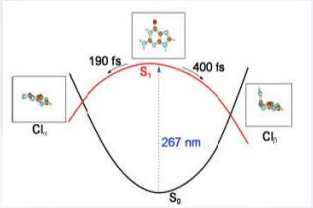

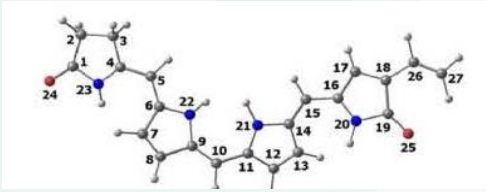

JCTC, 11, 1360,(2015); ***PCCP*** 19, 19168-19177 (2017)

Mapping Hamiltonian

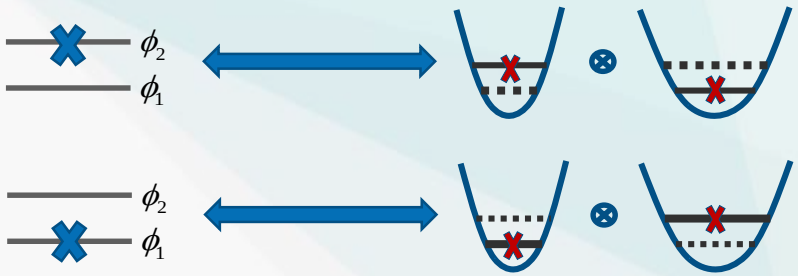

$$\hat{H} = \sum_{n,m} \hat{h}_{nm} |\phi_n\rangle\langle\phi_m|$$

$$|\phi_n\rangle\langle\phi_m| \mapsto a_n^+ a_m,$$
$$|\phi_n\rangle \mapsto |0_1 \cdots 1_n \cdots 0_N\rangle.$$

$$\hat{x}_n = (\hat{a}_n^+ + \hat{a}_n)/\sqrt{2}$$
$$\hat{p}_n = i(\hat{a}_n^+ - \hat{a}_n)/\sqrt{2}$$

$$\hat{H} = \sum_n \frac{1}{2}(\hat{x}_n^2 + \hat{p}_n^2 - 1)\hat{h}_{nn} + \frac{1}{2}\sum_{n\neq m}(\hat{x}_n\hat{x}_m + \hat{p}_n\hat{p}_m)\hat{h}_{nm}$$

Exciton Dynamics

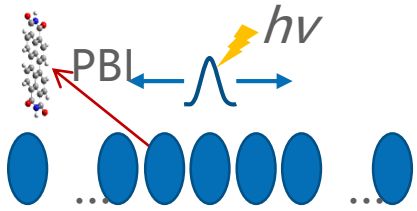

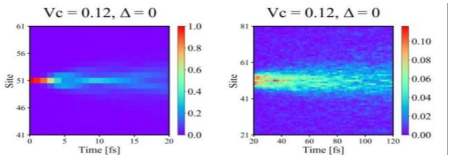

101 Sites, 808 Modes

Analysis Dynamics

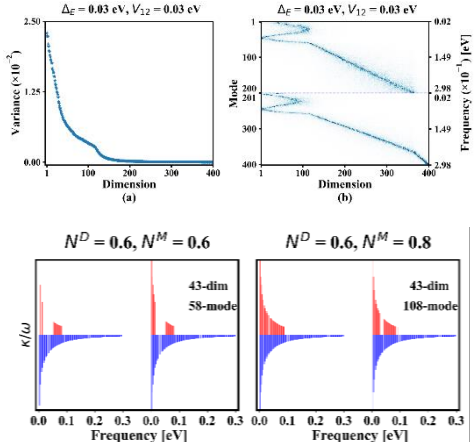

Which Modes are important?

On-the-fly Dynamics

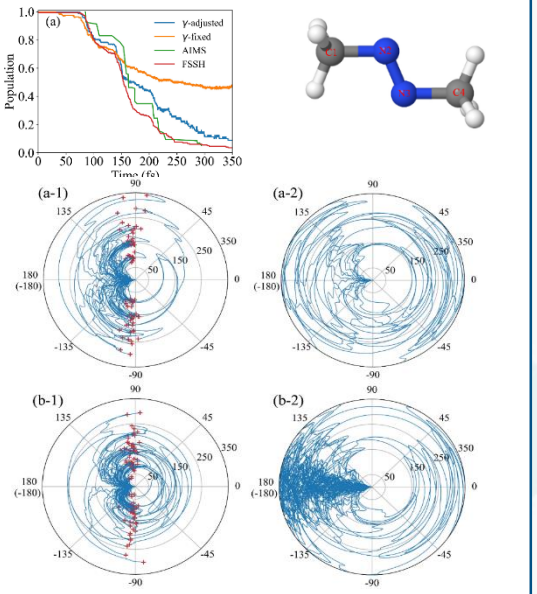

- ***JCP***, 2016, 2018; ***PCCP,*** 2019, 2020; ***JCTC***, 2021

Analysis of trajectory evolution I

- Dimensionality reduction approaches to analyze the surface-hopping dynamics simulation results
- Extract the major molecular motion

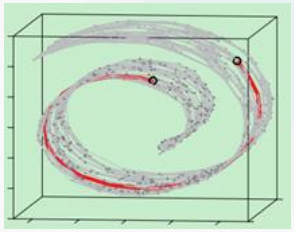

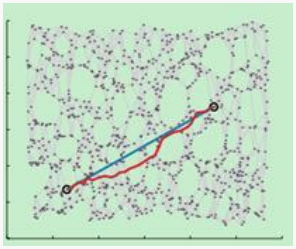

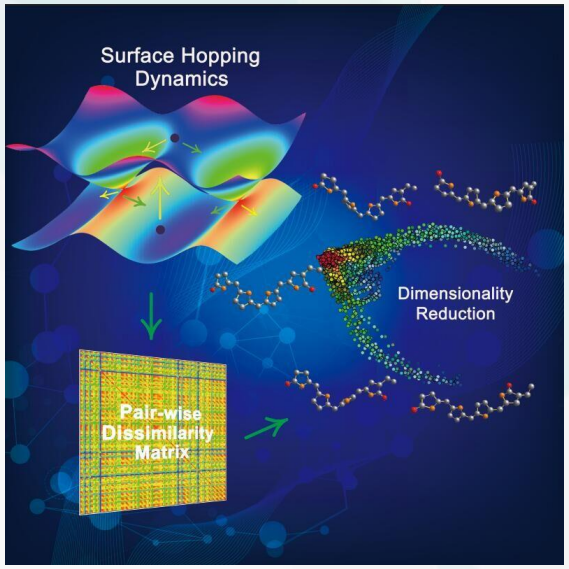

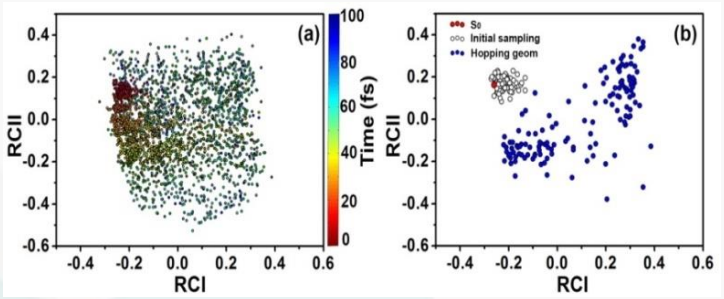

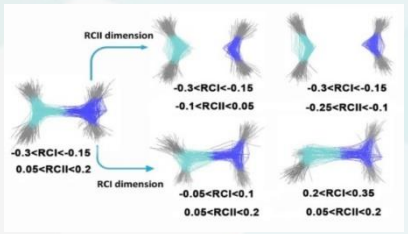

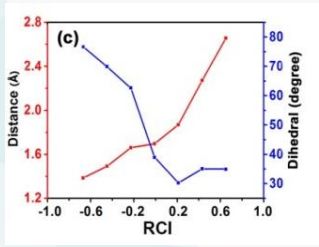

- **A large number of trajectories**
- **Polyatomic molecules**
- **Many degrees of freedom**

→

- **Multidimensional scaling**
- **Isometric feature mapping**

JCTC, 2017, 13, 4611−4623

Analysis of trajectory evolution II

- An "automatic" approach to analyze the trajectory similarity and the configuration similarity in the on-the-fly trajectory surface hopping dynamics.

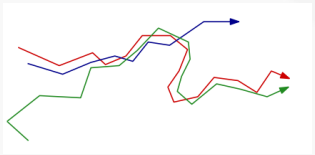

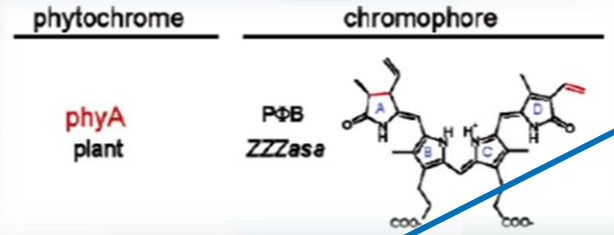

Fréchet Distance

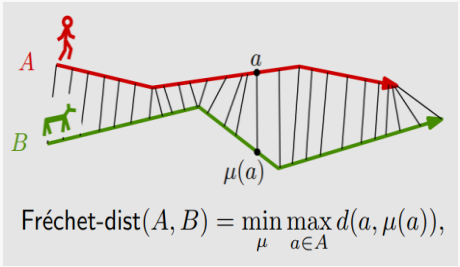

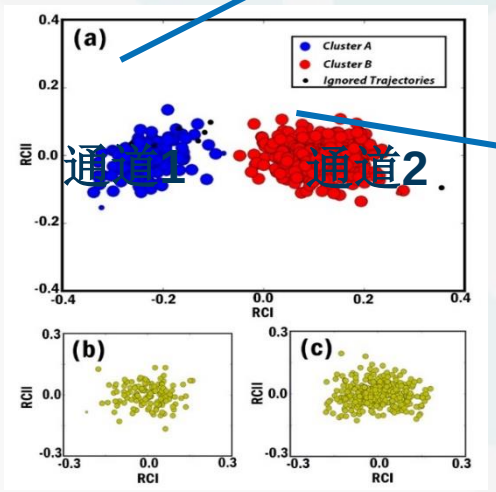

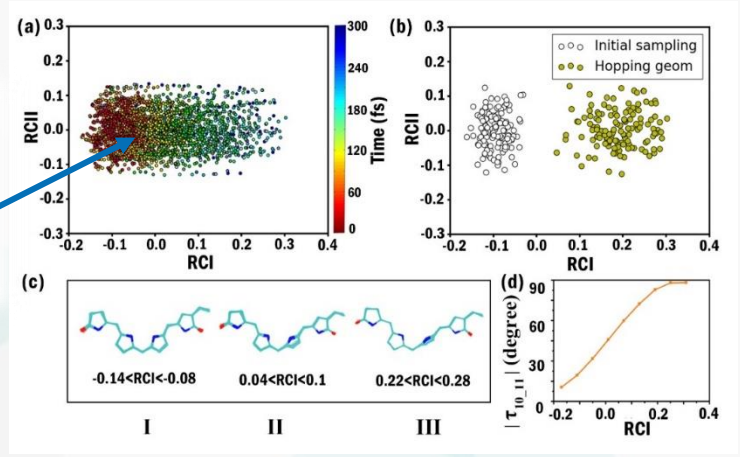

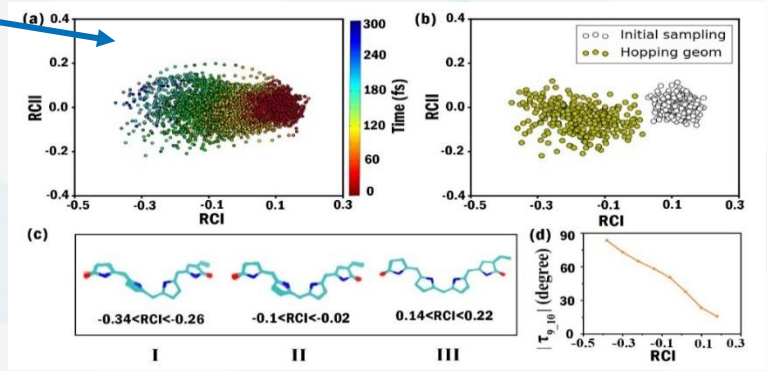

JCP 149, 244104 (2018)

Machine-Learning PES in nonadiabatic dynamics

- **The kernel ridge regression is used to build the excited-state PESs**
- **Nonadiabatic dynamics based on ML-PESs**

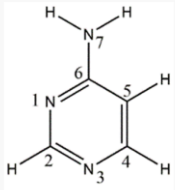

6-aminopyrimidine (6AP)

Coulomb Matrix

$$M_{kl} = \begin{cases} 0.5Z_k^{2.4} & k = l \\ \dfrac{Z_k Z_l}{\|R_k - R_l\|} & k \neq l \end{cases}$$

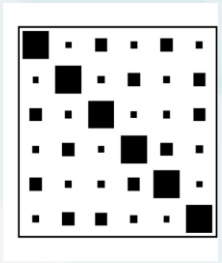

$$f(\boldsymbol{m}_i) = \sum_{j=1}^{N_t} \boldsymbol{c}_j \mathrm{K}(\boldsymbol{m}_i, \boldsymbol{m}_j)$$

$$\mathrm{K}(\boldsymbol{m}_i, \boldsymbol{m}_j) = \exp\left(-\frac{\|\boldsymbol{m}_i - \boldsymbol{m}_j\|^2}{2\sigma^2}\right)$$

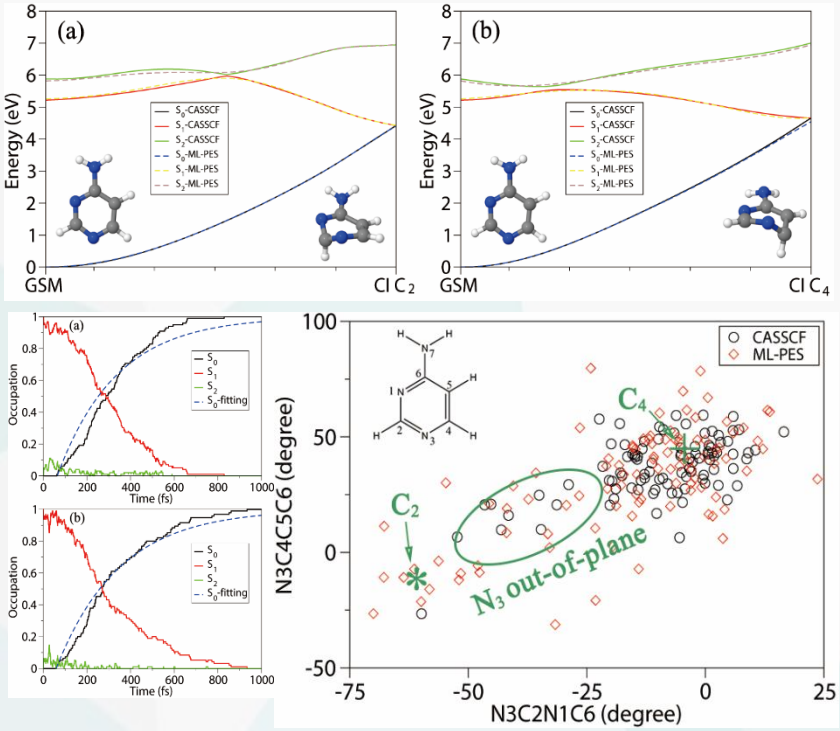

- **Achieve the efficient massive dynamics simulations with a large number of trajectories.**

JPCL 9, 2725-2732 (2018)

Exciton dynamics in OPV systems

- **Methodology： Vibronic Diabatic Hamiltonian, ML-MCTDH, Mapping Hamiltonian dynamics, Tensor Network**

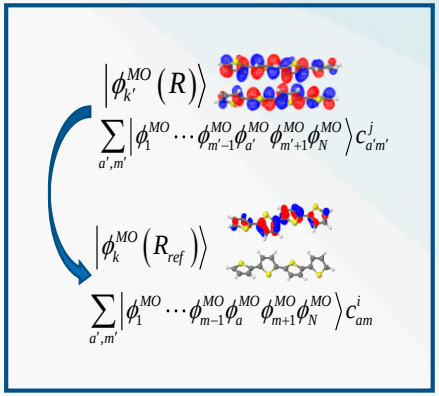

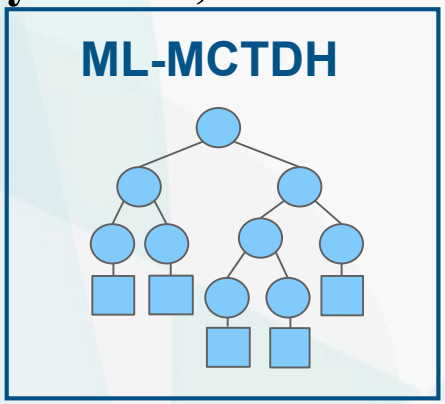

$$\hat{H} = \sum_{n,m} \hat{h}_{nm} |\phi_n\rangle\langle\phi_m|$$

$$\hat{H} = \sum_n \frac{1}{2}\left(\hat{x}_n^2 + \hat{p}_n^2 - 1\right)\hat{h}_{nn} + \frac{1}{2}\sum_{n\neq m}\left(\hat{x}_n\hat{x}_m + \hat{p}_n\hat{p}_m\right)\hat{h}_{nm}$$

- **Applications： Excited-state electron/energy transfer， Singlet fission**

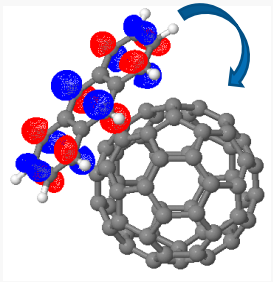

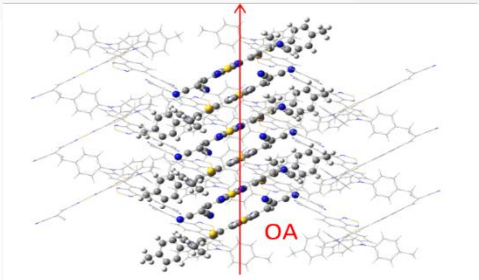

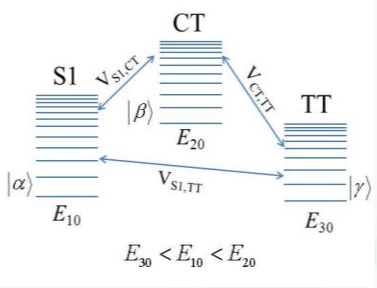

- **Role of Electron-phonon couplings**
- **Resonance effects**
- **Quantum coherences**

JCP 142, 084706 (2015); ***JPCC*** 120, 1375-1389 (2016); ***JPCC*** 121, 27263-27273 (2017); ***Chem. Phys.*** 515, 603 (2018); ***JPCA*** 121, 9567 (2017)

Acknowledgement and Starting

Guangzhou in China

City view of Guangzhou

South China Normal University

Funding: NSCF

Thanks my current and previous group members:

- Dr. Deping Hu, Mr. Jiawei Peng, Miss Kunni Lin,
- Mr. Qinghai Cui, Miss Juanjuan Zhang, Mr. Shichen Lin
- Dr. Yu Xie, Dr. Jie Zheng

Thanks my collaborators:

- Prof Maxim Gelin, Prof. Fenglong Gu, Prof. Chao Xu

New Postdoc and Research Assistant Positions are open !!!

Thank you!